nature communications

Article

https://doi.org/10.1038/s41467-025-59398-7

BRD4 modulator ZL0580 and LEDGINs additively block and lock HIV-1 transcription

Received: 8 April 2024

Accepted: 22 April 2025

Published online: 07 May 2025

Check for updates

Eline Pellaers[1], Julie Janssens[2], Lore Wils[1], Alexe Denis[1], Anayat Bhat[3], Siska Van Belle[1], Da Feng[4], Frauke Christ[1], Peng Zhan[4] & Zeger Debyser[1]

The persistence of HIV-1 in a latent state within long-lived immune cells remains a major barrier to a cure for HIV-1 infection. The "block-and-lock" strategy aims to silence the HIV-1 provirus permanently using latency promoting agents (LPAs). LEDGINs, a well-known class of LPAs, inhibit the interaction between viral integrase and LEDGF/p75, reducing viral integration and retargeting the provirus to regions resistant to reactivation. However, proximity to enhancers may still permit residual transcription. Given BRD4's central role in the enhancer biology, we now test two BRD4 modulators, JQ1 and ZL0580. Mechanistic studies reveal that JQ1 and ZL0580 have contrasting effects on Tat-dependent HIV-1 transcription, resulting in JQ1 promoting viral reactivation and ZL0580 inducing transcriptional silencing. Combining ZL0580 with LEDGINs has an additive effect in blocking HIV-1 transcription and reactivation, in both cell lines and primary cells. These findings demonstrate the potential of ZL0580 to enhance the block-and-lock cure strategy.

Combination antiretroviral therapy (cART), has turned HIV infection from a deadly into a chronic illness. While cART suppresses HIV replication to undetectable levels, a latent reservoir of immune cells with stably integrated HIV provirus persists[1]. Hence, cART requires lifelong therapy, concommitant with residual viremia further driving immune activation and inflammation leading to HIV-associated complications[2]. To cure HIV-1 infection the latent reservoir needs to be eradicated[3] or permanently silenced[4–9]. Initial efforts focused on eradicating infected cells using the shock-and-kill strategy[3,10–12]. However, challenges in clinical trials[3,13–16] shifted the interest to block-and-lock cure strategies in which the virus is pushed into a deep latent state by using latency promoting agents (LPAs)[3–10,17,18].

The Valente lab has targeted the viral protein Transactivator of transcription (Tat)[19,20], which recruits the positive transcription elongation factor b (P-TEFb) to the paused RNA polymerase II, enhancing viral transcription[21]. The Tat inhibitor, didehydrocortistatin A, was shown to prevent transcriptional elongation in latency cell line models, in primary cells from aviremic individuals, and in humanized mouse models[19,20,22]. Moreover, this effect persisted after treatment cessation for 25 days in human primary CD4$^+$ T cells and for 19 days in humanized mouse models by the induction of epigenetic modifications[20,22,23]. This is favorable in the block-and-lock cure strategy as it aims to induce a durable suppression of HIV-1 gene expression by administering LPAs as few times as possible, ideally once.

Although the Valente group first coined the term "block-and-lock"[22], LEDGINs were previously shown to induce deep latency in cell culture. The lens epithelium-derived growth factor (LEDGF/p75) directs HIV integration towards the methylated histone mark H3K36me2/3, ensuring active transcription[24–34]. Using structure-based drug design, small molecules were developed that bind to the LEDGF/p75 pocket of the viral integrase, named LEDGINs[35–40]. Using orthogonal approaches, LEDGINs were proven to reduce HIV-1 integration, shift integration towards the inner nucleus and retarget the provirus away from H3K36me2/3[38,40–43]. As such, LEDGINs hamper the transcriptional activity (block) and prevent reactivation from latency (lock) even after their removal. However, neither didehydrocortistatin A, nor LEDGINs by themselves suppress HIV-1 transcription completely and durably, underscoring the need for new LPA drug targets.

[1]Laboratory for Advanced Disease Modelling, Targeted Drug Discovery and Gene Therapy (ADVANTAGE), Herestraat 49, Leuven, Flanders, Belgium. [2]Department of Medicine, University of California San Francisco (UCSF), San Francisco, CA, USA. [3]Department of Microbiology, Washington University (WashU), Saint Louis, MI, USA. [4]Department of Medicinal Chemistry, Key Laboratory of Chemical Biology (Ministry of Education), School of Pharmaceutical Sciences, Shandong University, Jinan, China. e-mail: zeger.debyser@kuleuven.be

Using barcoded viruses, it was found that transcriptional activity of HIV correlates with proximity to the LEDGF/p75 mark H3K36me2/3 and enhancers[41]. While, LEDGINs shifted integration away from H3K36me2/3, still a small population of cells with high viral RNA (vRNA) expression persisted. Vansant et al. proved that these high vRNA expressing cells were integrated near enhancer sites, independently of LEDGINs[41]. Given bromodomain-containing protein 4 (BRD4)'s role in the enhancer biology[44,45], we now used BRD4 modulators to reinforce our LEDGIN-based block-and-lock cure strategy. However, BRD4 competes with Tat for P-TEFb during HIV-1 transcription, pausing the RNA polymerase II[46–50]. Most BRD4-modulators, among which JQ1 is a well-known example, reactivate HIV-1 transcription by binding to the acetyl-recognition pocket of BRD4 and as such displacing BRD4 from the viral promotor[46–50]. Niu et al. discovered the first BRD4 modulator, ZL0580, which suppresses HIV-1 transcription in latency cell line models and peripheral blood mononuclear cells (PBMCs) from HIV-infected individuals[51,52]. Co-immunoprecipitation (Co-IP) analysis and chromatin immunoprecipitation sequencing (ChIP-seq) with key factors in HIV transcriptional elongation proved that ZL0580 promotes the binding of BRD4 to the viral promotor, increasing competition with Tat for P-TEFb[51–53]. Still, the full mechanism of ZL0580 remains elusive.

To validate BRD4 as a drug target for a block-and-lock functional cure strategy, we investigated the inhibitory effect of ZL0580 on HIV-1 transcription in a side-by-side comparison with JQ1. Using luciferase reporter readouts in latency cell line models and PBMCs, we confirm that JQ1 promotes and ZL0580 suppresses HIV-1 transcription and reactivation. Interestingly, multiple pretreatments with ZL0580 extends inhibition of HIV-1 transcription after its removal from cell culture, indicating that the viral promotor may be epigenetically locked in a deep latent state. Next, we investigated the molecular mechanism of both BRD4 modulators. Using single-cell branched-DNA (bDNA) imaging we corroborate that JQ1 stimulates and ZL0580 inhibits HIV-1 transcription/reactivation without having an impact on viral DNA (vDNA) levels. Co-localization analysis shows that JQ1 suppresses and ZL0580 enhances the co-localization of BRD4 with acetylated histones. Moreover, JQ1 stimulates and ZL0580 inhibits Tat-dependent transcription in a HeLa-derived cell line harboring an integrated luciferase reporter gene under control of the HIV-1 promotor. Finally, ZL0580 additively silences HIV-1 transcription in combination with LEDGINs in latency cell line models and PBMCs infected in vitro. This is in line with our hypothesis that BRD4-driven enhancers may steer residual transcription after LEDGIN-treatment. To conclude, combining LEDGINs and ZL0580 increases the efficiency of the block-and-lock cure strategy. In addition, this study provides a preliminary assessment of the potential of BRD4 modulators as LPAs. However, for clinical application, the toxicity, potency and persistence of ZL0580 still require optimization.

Results

The BRD4 modulators JQ1 and ZL0580 have opposing effects on HIV-1 gene expression in latency cell line models

We assessed the effect of JQ1 and ZL0580 (Fig. 1a) on HIV-1 transcription and on cell viability in parallel in SupT1 cells. To this end, SupT1 cells were transduced with replication-deficient (single-round) NL4.3-based HIV-1 virus encoding luciferase, further referred to as HIV-1 FLuc virus. 3 days post-transduction, the residual virus was washed away, and cells were subcultured for an additional 7 days to allow silencing to occur. On day 10 post-transduction, a dilution series of compounds was added to the cells. Half of the wells were additionally reactivated with 10 ng/mL tumor necrosis factor alpha (TNF-α). Finally, 24 h post-reactivation, samples were harvested for the luciferase assay, flow cytometric analysis, and the MTT assay, as illustrated in Fig. 1b. Using luciferase as a readout, we investigated the effect of JQ1 and ZL0580 on HIV-1 transcription. JQ1 increased LTR-driven luciferase reporter expression in non-reactivated and TNF-α reactivated cells, with the stimulation reaching its maximum at 1 μM JQ1 (Fig. 1c). Relative luciferase expression was calculated by dividing the protein-normalized luciferase counts of the untreated controls by those of the JQ1-treated cells, separately for non-reactivated and TNF-α reactivated cells. This calculation indicated that 1 μM JQ1 approximately increased basal transcription to 250% and reactivation to 150% compared to respectively the non-reactivated and reactivated untreated control, shown at 100% (Fig. 1d). As JQ1 does not reactivate dose-dependently but reaches a maximum at 1 μM, no IC_{50} could be calculated. Paradoxically, ZL0580 dose-dependently suppressed the expression of the luciferase reporter gene in both non-reactivated and TNF-α stimulated cells (Fig. 1e). The IC_{50} of ZL0580 was calculated at 6.43 ± 0.34 μM in the non-reactivated cells and 4.14 ± 0.37 μM in the TNF-α reactivated cells (Fig. 1f).

In parallel cells were stained with propidium iodide and analyzed with flow cytometry to determine the toxicity. JQ1 did not affect cell viability at the concentrations used (Fig. S1a). However, ZL0580 showed toxicity from concentrations starting at 5 μM. The CC_{50} value of ZL0580 was estimated at 11.36 ± 0.55 μM and 10.89 ± 0.42 μM in non-reactivated and reactivated cells, respectively (Fig. S1b). As such, a selectivity index (SI) of ZL0580 was calculated at 1.77 ± 0.13 and 2.63 ± 0.26 in non-reactivated and reactivated cells. Because propidium iodide staining only detects late-stage membrane damage, additional toxicity studies were performed using the MTT assay, which measures metabolic activity. Non-infected SupT1 cells were incubated with a dilution series of ZL0580 for 24 h, and a CC_{50} of 9.65 ± 1.02 μM was calculated (Fig. S1c). Additionally, cells were infected, treated with ZL0580, and reactivated according to the protocol outlined in Fig. 1b. The MTT assay was performed on day 11 post-transduction. For this protocol, a CC_{50} of 7.06 ± 0.37 μM was calculated for non-reactivated cells, and 8.53 ± 0.45 μM for reactivated cells (Fig. S1d), resulting in a SI of 1.10 ± 0.08 and 2.06 ± 0.21 in non-reactivated and reactivated cells respectively. In Fig. S1e–f, the activity of ZL0580, measured by luciferase reporter expression, is overlaid with its toxicity, assessed using propidium iodide staining and the MTT assay. The toxicity data indicate that in non-reactivated cells, the concentrations at which ZL0580 is active are close to those at which it exhibits toxicity (Fig. S1e). However, for reactivated cells, the reduction in LTR-driven luciferase activity is more pronounced compared to the impact on cell viability (Fig. S1f). Notably, at concentrations between 2.5-7.5 μM, a significant decrease in HIV transcription is observed, while cytotoxicity remains relatively low (Fig. S1f). This indicates that the LPA effect after reactivation is specific to HIV-1 transcription. Moreover, in our assay, the luciferase counts were normalized to the total protein concentration, determined with the bicinchoninic acid (BCA) assy. To confirm that this normalization is accurate at high concentrations of ZL0580, we normalized both the cell viability (determined with propidium iodide staining and the MTT assay) and the protein level (determined with BCA assay) of the ZL0580-treated cells to those of the untreated control. This calculation indicated that the cell viability and protein levels decreased equally with ZL0580 treatment, proving that normalizing the luciferase counts for the total protein concentration is a correct method to take the toxicity of ZL0580 into account (Table S1).

Furthermore, to address the low selectivity index (SI) of ZL0580 and demonstrate that its effects in the luciferase reporter assays are HIV specific rather than a result of toxicity, less toxic analogues were generated. One such analogue, compound 24, was administered to SupT1 cells following the protocol outlined in Fig. 1b. Compound 24 showed a dose-dependent reduction in both HIV-1 transcription (IC_{50} = 5.48 ± 1.59 μM) and reactivation (IC_{50} = 5.66 ± 1.13 μM) (Fig. S2a). Notably, in the MTT assay, the compound did not reach its CC_{50}, even at the highest tested dose of 100 μM (Fig. S2b). In Fig. S2c–d, the LPA activity is overlaid with toxicity data, clearly showing that compound 24 inhibits HIV-1 transcription and reactivation without significantly

https://doi.org/10.1038/s41467-025-59398-7

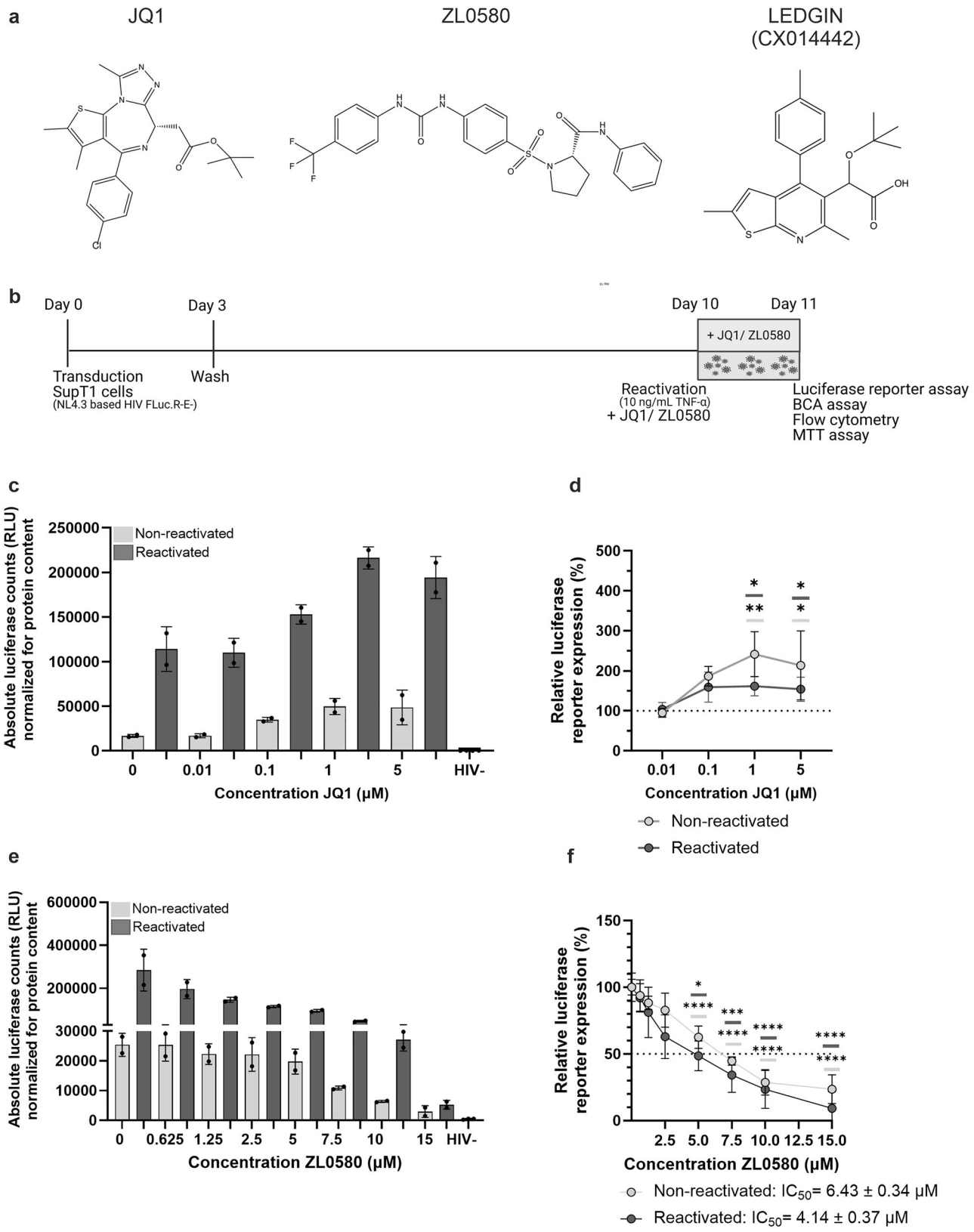

affecting cell viability. These findings support the notion that the effects of ZL0580 are not solely attributable to toxicity, as the analogue exhibits significantly reduced toxicity while maintaining similar LPA activity. However, further investigation into the potential of compound 24 in the block-and-lock cure strategy is beyond the scope of this paper.

The effect of ZL0580 on HIV latency was tested additionally in J-Lat A2 cells, a latently infected Jurkat cell line with a LTR-Tat-GFP cassette. J-Lat A2 cells were treated with ZL0580 and TNF-α for 24 h and HIV transcription was monitored by the percentage (%) of GFP$^+$ cells via flow cytometry. Alongside, cell viability was determined using a fixable viability dye. ZL0580 suppressed HIV-1 reactivation with an

Fig. 1 | JQ1 promotes and ZL0580 inhibits HIV-1 transcription and reactivation in SupT1 cells. a Chemical structure of JQ1, ZL0580 and LEDGIN (CX014442). **b** SupT1 cells were transduced with HIV-1 FLuc virus. After 3 days, residual virus was washed away. At day 10 post-transduction, a dilution series of JQ1 or ZL0580 was added to the wells and half of the wells were additionally reactivated with 10 ng/mL TNF-α. 24 h post-reactivation, samples were harvested for the luciferase assay, flow cytometric analysis and MTT assay. **c, e** Luciferase counts were normalized for the total concentration of protein (determined with BCA assay). Luciferase counts are presented for non-reactivated (light grey) and reactivated (dark grey) cells, for each concentration of JQ1 (**c**), or ZL0580 **e** with the non-transduced cells (HIV-) as a negative control. Each dot represents one biological duplicate. Mean ± SD of biological duplicates from 1 representative experiment out of 14 for JQ1 (n = 2) and 1 out of 15 for ZL0580 ($n = 2$) are shown. Statistics were not performed due to a limited number of data points. **d, f** Relative luciferase reporter expression (%) was calculated by dividing the luciferase counts normalized for protein content (BCA assay) from compound-treated cells by those from the control (0 μM ZL0580). This was calculated separately for non-reactivated (light grey) and reactivated cells (dark grey) for each concentration of JQ1 (**d**) or ZL0580 (**f**). The IC_{50}, 6.43 ± 0.34 μM and 4.14 ± 0.37 μM for non-reactivated and reactivated cells respectively, was calculated by a four-parameter logistic regression of a dose-response curve. Mean ± SD of biological duplicates from 3 representative experiments out of 14 for JQ1 ($n = 6$) and 3 out of 15 for ZL0580 ($n = 6$) are shown. Statistical significance was calculated with a One-Way ANOVA (two-sided test; Dunnett's multiple comparison test) between the compound-treated cells compared to the untreated control, separately for non-reactivated and reactivated cells (ns non-significant; * $p < 0.05$; ** $p < 0.01$;*** $p < 0.0001$; **** $p < 0.0001$). Source data are provided in the source data file. BCA, bicinchoninic acid; HIV-, non-transduced negative control; IC_{50}, 50% inhibitory concentration; ns, non-significant; RLU, relative light units; TNF-α, tumor necrosis factor α.

IC_{50} of 10.04 ± 0.38 μM. Viability was reduced at concentrations starting from 10 μM, giving a CC_{50} of 12.14 ± 0.31 μM. Despite a small therapeutic window (SI = 1.21 ± 0.06 μM), ZL0580 reduced HIV-1 reactivation at non-toxic levels (2.5-7.5 μM), showing again that its LPA effect wasn't solely due to toxicity (Fig. S3a). Gating strategy is presented in Fig. S3b.

Persistence of the effect of JQ1 but not ZL0580 after compound removal in SupT1 cells

In the block-and-lock cure strategy, LPAs must induce a durable suppression of HIV-1 gene expression. To verify if these BRD4 modulators may have long-term effects on HIV latency, we performed infection experiments in which we monitored gene expression after compound removal. The timeline of the infection experiment is described in the method section and illustrated in detail in Fig. S4a. First, we tested the persistent effect of JQ1. In accordance with Fig. 1c, JQ1 promoted HIV-1 transcription and reactivation, peaking at 1 μM on day 11 (Fig. S4b). In non-reactivated cells, this effect persisted dose-dependently after JQ1 removal (Fig. S4b). However, no promotion of TNF-α-induced reactivation was detected after JQ1 removal (Fig. S4c). Cell viability, assessed by propidium iodide staining and flow cytometry, showed no toxicity after addition of JQ1, both on day 11 and 13 post-transduction (Fig. S4d). Similar experiments with ZL0580 showed a dose-dependent decrease in HIV-1 basal transcription before its removal, but the effect did not persist after its removal (Fig. S5a). The inhibitory effects of ZL0580 on reactivation only persisted after treatment with 10 μM ZL0580 (Fig. S5b), likely due to toxicity (Fig. S5c). Collectively, these results demonstrate the ability of JQ1 to maintain a stimulatory effect under non-reactivated conditions after withdrawal from cell culture, while ZL0580's inhibition did not persist at non-toxic doses.

JQ1 and ZL0580 have distinct molecular mechanisms of action

We demonstrated that JQ1 and ZL0580, two BRD4-targeting molecules, have opposite effects on HIV-1 transcription (Fig. 1). To explore their mechanisms, we used 3 approaches. First, we identified which part of the HIV-1 replication cycle is blocked using bDNA imaging, a cutting-edge technique which detects vDNA and vRNA simultaneously to distinguish pre- or post-integration blocks. Second, we assessed BRD4 binding to acetylated histones by measuring its co-localization with the acetylation markers H3K9/14Ac[31] and H4K8Ac[54] via confocal microscopy. Third, we examined their impact on Tat-dependent transcription using a HeLa-derived cell line with an 5'LTR-driven luciferase reporter gene, referred to as HeLa-TZMbl. Cell culture experiments were performed as described in Fig. 1b. Cells harvested on day 11 post-transduction were fixed, permeabilized, and hybridized with target-specific Z-probes for vDNA or vRNA detection. Amplifiers conjugated with fluorophores allowed confocal imaging (Figs. S6a and S7a). An in-house MATLAB routine was used to calculate vDNA and vRNA levels per single cell. JQ1 treatment had no impact on the vDNA level in either non-reactivated or reactivated cells (Fig. S6b and Table S2). Only infected cells, which contain vDNA and/or vRNA copies, were included in the analysis of transcription. JQ1 treatment of non-reactivated and reactivated cells increased vRNA expression, peaking at 1 μM, corroborating its latency reactivating activity (Fig. 2a and Table S2). To correct for differences in HIV-1 infectivity, vRNA expression levels were normalized for vDNA levels. For both the non-reactivated and reactivated cells, this ratio reached an optimum at 1 μM JQ1. At a higher concentration of JQ1 (5 μM), the ratio in the non-reactivated cells decreased modestly, while a more pronounced decrease was seen in the reactivated cells (Fig. 2b and Table S2).

To statistically evaluate JQ1's effect on HIV-1 transcription, a negative binomial model was used as it is capable of fitting over-dispersed data (Fig. S6c). The outcome variable, vRNA spots per infected cell, was dependent on the concentration of JQ1 and the reactivation of the cells. The odds ratio (OR) for the non-reactivated cells treated with 0.2 μM, 1 μM, and 5 μM JQ1 was 1.28, 4.28, and 3.74, respectively ($p < 0.005$ for 1 and 5 μM). This indicated an increase of 28%, 328%, and 274% in the vRNA spots for the non-reactivated cells treated with 0.2 μM, 1 μM, and 5 μM JQ1, respectively, compared to the non-reactivated untreated control (Fig. S6c). TNF-α reactivation increased the OR by 250% compared to non-reactivated untreated cells. The highest OR after reactivation was 1.80 for cells treated with 1 μM JQ1, although the interaction term was not significant (Fig. S6c). For ZL0580, low ZL0580 concentrations (1.25 μM, 2.5 μM) kept the vDNA levels constant, while higher concentrations (5 μM, 7.5 μM) increased the vDNA spots, likely due to toxicity (Fig. S7b**;** Table S3). ZL0580 significantly reduced HIV-1 transcription and reactivation, as indicated by a dose-dependent decrease in vRNA expression (Fig. 2c**;** Table S3). ZL0580 also reduced vRNA expression per vDNA copy in non-reactivated and TNF-α reactivated cells (Fig. 2d**;** Table S3). The negative binomial model showed a highly significant ($p < 0.001$) OR of 0.2 for both 5 μM and 7.5 μM ZL0580, indicating an 80% decrease in vRNA spots per infected cell compared to the untreated control. The ORs for reactivated cells treated with ZL0580 were 0.38, 0.41, 0.16, and 0.28 for 1.25 μM, 2.5 μM, 5 μM, and 7.5 μM, respectively (Fig. S7c).

To investigate the distinct effects of JQ1 and ZL0580, co-localization was measured of BRD4 with the acetylation markers H3K9/14Ac and H4K8Ac, showing a high affinity for BRD4[31,54]. JQ1 is known to bind to the KAc pocket of BRD4, dissociating it from H3K9/14Ac, while ZL0580 binds to a non-KAc pocket, enhancing BRD4's interaction with acetylated histones[51,55]. Co-localization was quantified using Pearson's correlation coefficient (PCC), where 0 indicates no correlation and 1 indicates a perfect correlation. The untreated control showed a PCC of 0.73 ± 0.09 (mean ± SD) of BRD4 with H3K9/14Ac, which decreased to 0.60 ± 0.06 after JQ1 treatment (1 μM) but increased to 0.81 ± 0.06 after ZL0580 treatment (3.4 μM) (Fig. 2e). For H4K8Ac, the PCC was 0.79 ± 0.09 in the control, dropping to

https://doi.org/10.1038/s41467-025-59398-7

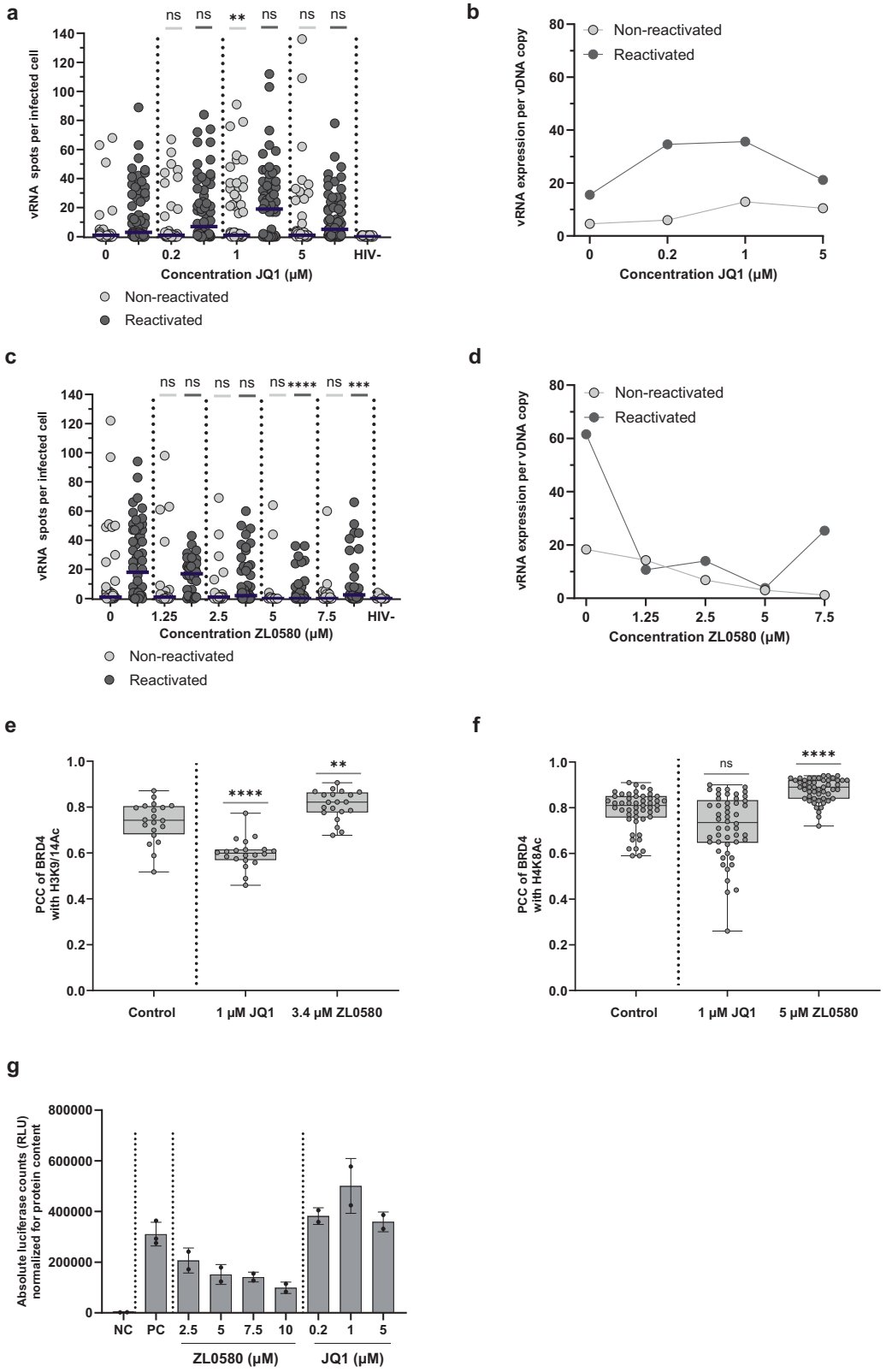

0.72 ± 0.14 after addition of JQ1 and rising to 0.88 ± 0.05 after addition of ZL0580 (Fig. 2f). These results confirm that JQ1 and ZL0580 have opposite effects on BRD4 binding to acetylated histones.

Additionally, we investigated the role of the viral protein Tat using an HeLa-derived cell line containing an integrated luciferase reporter gene driven by the 5′-LTR solely. After transfecting with the Tat plasmid, cells were treated for 24 h with varying concentrations of JQ1 or ZL0580. Tat transfection increased luciferase expression 133-fold compared to the negative control. ZL0580 decreased luciferase activity in a dose-dependent manner compared to the positive control. In contrast, 1 μM JQ1 enhanced luciferase expression by 1.6-fold relative to the positive control (Fig. 2g). To rule out the possibility that the observed phenotype resulted from toxicity, cell viability was assessed in HeLa-TZMbl cells following transfection and treatment with ZL0580

Fig. 2 | JQ1 and ZL0580 have distinct molecular mechanisms of action. a–d Cells were treated with JQ1 **(a,b)** or ZL0580 **(c, d)** following Fig. 1b and harvested for bDNA imaging on day 11. **a, c** The number of vRNA spots per infected cell were plotted. Each dot represents a single cell, with a dark blue bar indicating the median. **b, d** vRNA expression was normalized to vDNA expression. Table S5 shows the number of cells imaged. **a, b** For JQ1, 86 cells were imaged in each condition ($n = 86$). **c, d** For ZL0580, 100 cells were imaged in each condition except for HIV- in which 61 cells were imaged ($n = 100$). Results from 1 representative experiment out of 4 for JQ1 and 1 out of 2 for ZL0580 are shown. A Kruskal-Wallis test (two-sided test; Dunnett's multiple comparison test) compared compound-treated cells to the untreated control, separately for non-reactivated and reactivated cells (ns non-significant; * $p < 0.05$; ** $p < 0.01$; *** $p < 0.0001$; **** $p < 0.0001$). **e, f** SupT1 cells were treated for 24 h with JQ1/ZL0580. Cells were incubated with primary anti-BRD4, anti-H3K9/14Ac (**e**) and anti-H4K8Ac (**f**) antibodies. The line in the box represents the median. The top and bottom lines of the box are the first and third quartiles. The top and bottom winkers are the minimum and maximum PCC value. Each dot represents a single cell. 20 cells were imaged for (**e**) ($n = 20$) and 50 cells for (**f**) ($n = 50$). Results from 1 representative experiment out of 1 for (**e**) and 1 out of 2 for (**f**) are shown. A Kruskal-Wallis test (two-sided test; Dunnett's multiple comparison test) (**e**) and One-Way ANOVA test (two-sided test; Dunnett's multiple comparison test) (**f**) compared the PCC value of the compound-treated cells to the control (ns non-significant; * $p < 0.05$; ** $p < 0.01$; *** $p < 0.0001$; **** $p < 0.0001$). **g** HeLa-based TZMbl cells were transfected with a Tat plasmid and treated for 24 h with JQ1/ZL0580 or DMSO. NC represents the negative control not transfected with Tat plasmid and PC the positive control transfected with Tat plasmid but treated with DMSO. Luciferase counts, normalized for the total concentration of protein (BCA assay), were plotted. Each dot represents one biological duplicate. Mean ± SD of biological duplicates from 1 representative experiment out of 3 are shown ($n = 2$). Statistics were not performed due to a limited number of data points. Source data are provided in the source data file. BCA bicinchoninic acid protein assay, BRD4 bromodomain containing protein 4, HIV- non-transduced negative control, NC negative control, ns non-significant, PC positive control, PCC Pearson Correlation Coefficient, RLU relative light units, Tat trans-activator of transcription, TNF-α tumor necrosis factor α, vDNA viral DNA, vRNA viral RNA.

and JQ1 using the MTT assay. ZL0580 exhibited clear toxicity only at a concentration of 15 µM (Fig. S8a), whereas JQ1 demonstrated no detectable toxicity in the cell line tested (Fig. S8b). These findings underscore the essential role of Tat in the mechanisms of JQ1 and ZL0580 and illustrate their opposing effects on Tat-dependent transcription. Furthermore, this confirms that the LPA effect of ZL0580 is HIV-1 transcription specific.

The effect of BRD4 modulators on LEDGIN-retargeted proviruses in SupT1 cells

LEDGINs have been proven to block and retarget HIV integration, resulting in transcriptionally silent proviruses that are refractory to reactivation[38,40–42]. However, single-cell studies indicate that some cells maintain high levels of viral transcription[41,42]. Using barcoded viruses, we proved that these high vRNA expressing cells are integrated close to enhancers[41]. We hypothesized that combining enhancer antagonists with LEDGINs would completely silence HIV-1 gene expression. Given BRD4's role in enhancer biology[44,45], we hypothesized that BRD4 modulators could block the residual transcriptional activity of LEDGIN-retargeted proviruses. Thus, we combined JQ1 and ZL0580 with LEDGINs in cell line models. First, the effect of LEDGIN CX014442 (Fig. 1a) on HIV-1 infectivity was assessed. We have already confirmed this in previous publications[38,40–42], but here the aim was 3-fold: 1) determine the IC_{50} of our CX014442 stock; 2) confirm that CX014442 blocks integration and reduces HIV-1 transcription; and 3) verify that high concentrations of CX014442 still allow for persistent high vRNA expression in some cells. SupT1 cells were treated with CX014442 during transduction with the HIV-1 FLuc virus. Three days later, the inhibitory effect of CX014442 on HIV-1 infectivity was assessed with the luciferase assay, determining an IC_{50} of 4.05 ± 0.44 µM (Fig. 3a). Concentrations ranging from 2.35 µM to 18.83 µM, equivalent to 0.58-4.65 x IC_{50}, were used to determine the effect of CX014442 on HIV-1 latency and reactivation. As LEDGINs target viral integration, CX014442 was added to the SupT1 cells during transduction according to the protocol described in Fig. 3b but without the addition of JQ1/ ZL0580 on day 10. Propidium iodide staining on day 3 indicated that CX014442 did not affect cell viability (Fig. 3c). The luciferase assay on day 11 post-transduction proved that LEDGINs dose-dependently block LTR-driven luciferase reporter expression in the non-reactivated and TNF-α-reactivated cells (Fig. 3d). Next, bDNA imaging was conducted. Quantitative analysis of the vDNA spots showed that the addition of CX014442 significantly decreased the vDNA levels (Fig. 3e; Table 1). Evaluation of the vRNA levels proved that treatment with CX014442 dose-dependently hampered HIV-1 basal transcription and reactivation (Fig. 3f; Table 1). A significant OR of 0.2 ($p < 0.001$) was calculated at 18.83 µM CX014442 with the negative binomial probability distribution, indicating an 80% reduction in vRNA levels compared to the untreated control. The OR of the reactivated cells treated with 18.83 µM CX014442 was equal to 0.12 (Fig. S9). Despite significant reductions in basal transcription and reactivation, single-cell analysis revealed that 3 cells with high vRNA expression persisted at the highest CX014442 concentration (18.83 µM) (Fig. 3f), likely due to residual integration near enhancer sites regulated by BRD4. Future experiments aim to completely silence viral expression by combining BRD4 modulators with LEDGINs.

Next, we investigated the effect of JQ1 and ZL0580 on CX014442-retargeted proviruses using single-round infections as described in Fig. 3b. To investigate the impact of JQ1 on LEDGF/p75-targeted *vs.* LEDGIN-retargeted proviruses, the luciferase counts on day 11 post-transduction were normalized to the control condition (0 µM JQ1) for each concentration of CX014442. At the optimal JQ1 concentration of 1 µM, there was a significant increase to ± 400% in luciferase reporter expression compared to the control (0 µM JQ1), which was independent of CX014442 pretreatment (Fig. 4a). The Combenefit model creates a 3D model of the luciferase counts normalized to the untreated control (0 µM CX014442 and JQ1)[56]. In addition, synergy scores were calculated by comparing the Bliss-model-generated dose-response surface, for which an additive effect is expected, with the experimental dose-response surface. Scores below -10 indicate antagonism (shown in red), scores between -10 and 10 indicate additivity (green), and scores above 10 indicate synergy (blue). As anticipated, antagonistic drug-drug interactions were observed at low CX014442 concentrations (2.35-4.7 µM CX014442) and high JQ1 concentrations (1-5 µM JQ1) (Fig. 4b). Notably, after using high CX014442 concentrations (9.42-18.83 µM CX014442), which significantly retargets the provirus to transcriptionally silent chromatin, JQ1 and CX014442 exhibited less antagonism (Fig. 4b). Upon TNF-α-mediated reactivation, JQ1 enhanced viral transcription in cells treated with varying CX014442 concentrations (± 200% at 1 µM JQ1) (Fig. 4c). Combenefit analysis also showed that JQ1 acted antagonistically at low concentrations of CX014442 and that a switch occurred to more additive scores at higher concentrations of CX014442 (Fig. 4d). In conclusion, the LPA CX014442 and the LRA JQ1 act as antagonists. However, at high LEDGIN concentrations, the LPA activity of JQ1 surpasses its LRA activity, probably reflecting the altered chromatin environment of the retargeted provirus.

In addition, we tested the combination of the LPAs ZL0580 and CX014442. CX014442 was combined with ZL0580, according to the protocol described in Fig. 3b. In the luciferase assay, ZL0580 significantly reduced HIV-1 transcription with and without CX014442-treatment (± 80% inhibition at 10 µM ZL0580) (Fig. 5a). The 3D model shows an almost complete absence of luminescence after combination treatment with high concentrations of ZL0580 (10 µM) and CX014442 (18.83 µM). Moreover, synergy calculations using the Combenefit

https://doi.org/10.1038/s41467-025-59398-7

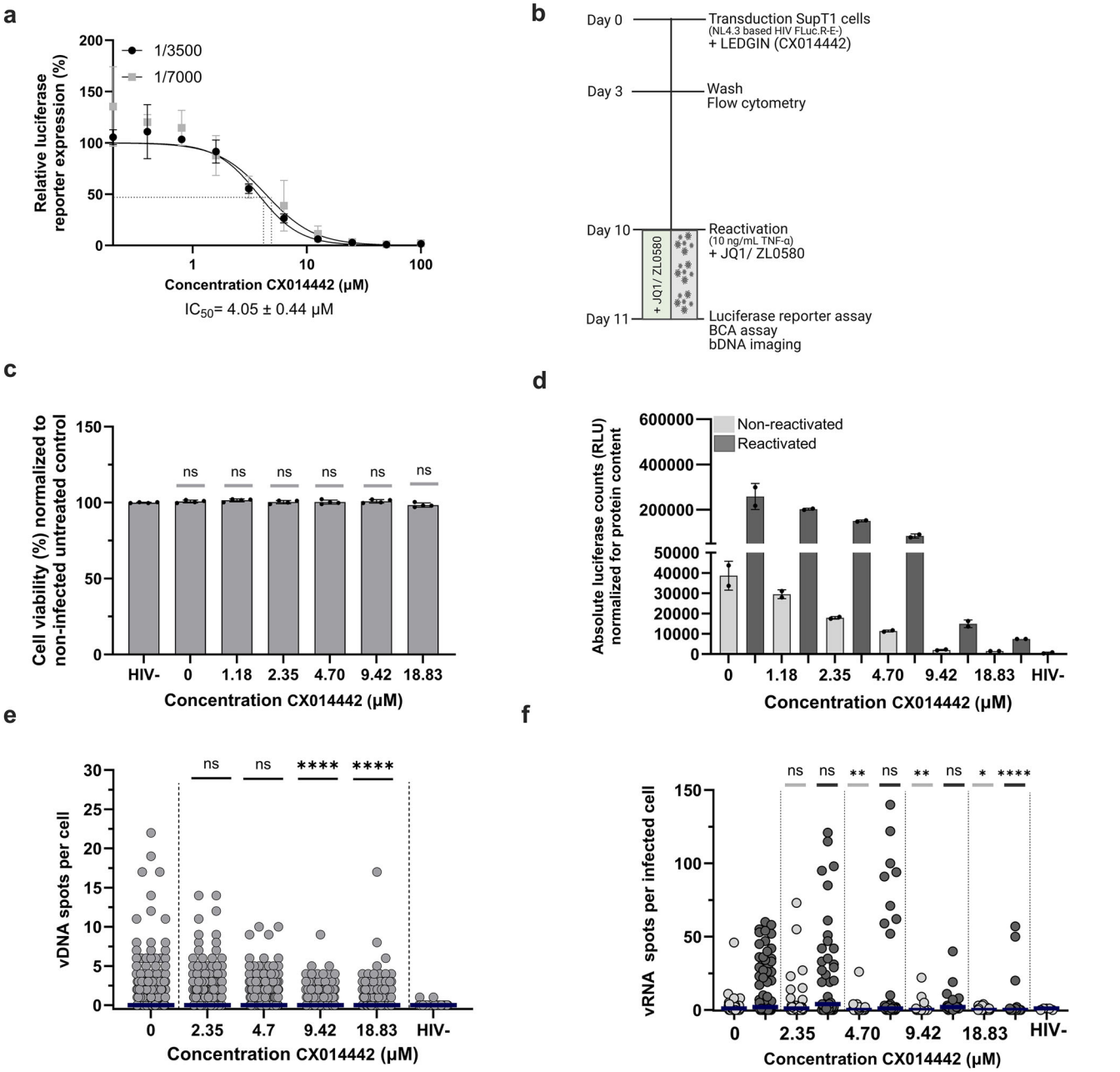

Fig. 3 | LEDGIN CX014442 inhibits HIV-1 integration and hampers HIV-1 transcription and reactivation in SupT1 cells. a SupT1 cells were transduced with HIV-1 FLuc virus and treated with CX014442 for 3 days. The IC_{50}, 4.05 ± 0.44 µM, was determined using a four-parameter logistic regression of a dose-response curve of the relative luciferase reporter expression (%). Mean ± SD of biological duplicates of 1 independent experiments out of 2 are presented ($n = 2$). **b** SupT1 cells were transduced with HIV-1 FLuc virus and treated with CX014442. On day 3, cells were washed and assessed for toxicity. On day 10, cells were reactivated with TNF-α (10 ng/mL) and treated with JQ1/ZL0580. After 24 h, luciferase assays and bDNA imaging were performed. **c** Cell viability was analyzed via propidium iodide staining on day 3, normalized to non-infected untreated controls, and compared to HIV- (NC) via a One-Way ANOVA test (two-sided test; Dunnett's multiple comparison test; ns, non-significant). Each dot represents one biological duplicate. Mean ± SD of 2 biological duplicates of 2 independent experiments out of 2 are presented ($n = 4$). **d** Luciferase counts (normalized to protein content; BCA assay) are presented for cells harvested on day 11. Each dot represents one biological duplicate. Mean ± SD of 2 biological duplicates of 1 independent experiments out of 2 are presented ($n = 2$). Statistics were not performed due to a limited number of data points. **e, f** The vDNA spots per cell **(e)** and the vRNA spots per infected cell **(f)** were determined with bDNA imaging. vDNA spots of non-reactivated and reactivated cells and cells treated with different concentrations of JQ1 were pooled if treated with the same concentration of CX014442. VRNA spots were not pooled. Each dot represents a single cell, with a dark blue bar indicating the median. Table S5 shows the number of cells imaged per condition. For vDNA detection, 900 cells were imaged in each condition ($n = 900$). For vRNA detection, 100 cells were imaged for each condition ($n = 100$). Except for HIV-, 37 cells were imaged for vDNA and vRNA detection. Results from 1 representative experiment out of 2 are shown. A Kruskal-Wallis test (two-sided test; Dunnett's multiple comparison test) compared the vDNA/ vRNA spots of the CX014442-treated cells to those of the control (ns non-significant; * $p < 0.05$; ** $p < 0.01$; *** $p < 0.0001$; **** $p < 0.0001$). Source data are provided in the source data file. HIV-, non-transduced negative control; IC_{50}, 50% inhibitory concentration; NC, negative control; ns, non-significant; TNF-α, tumor necrosis factor α; vDNA, viral DNA; vRNA, viral RNA.

https://doi.org/10.1038/s41467-025-59398-7

Table 1 | Viral DNA and RNA levels after CX014442 treatment

Concentration CX014442 (μM)	vDNA detection ($n = 900$)		vRNA detection ($n = 100$)			
	Pooled		Non-Reactivated		Reactivated	
	Total vDNA spots	% infected	Total vRNA spots	% vRNA$^+$ cells	Total vRNA spots	% vRNA$^+$ cells
0 (control)	606	29.11	139	34.00	1039	57.00
2.35	475	25.11	254	29.00	1038	34.00
4.70	462	28.33	57	19.00	836	33.00
9.42	229	16.22	38	5.00	135	33.00
18.83	293	19.00	28	18.00	131	6.00
HIV- (NC)			3	8.11		

Cells were transduced with HIV-1 FLuc virus and treated with CX014442/JQ1 according to the timeline presented in Fig. 3b. The left part of the table shows the total number of vDNA spots and the % of infected cells. For viral DNA detection, cells treated with different concentrations of JQ1, and non-reactivated and reactivated cells were pooled, if they were treated with the same concentration of CX014442. The right part shows the total number of vRNA spots and the percentage of cells that contain vRNA spots per condition. No conditions were pooled for the calculation of the vRNA levels. Table S5 shows the number of cells imaged per condition. For vDNA detection, 900 cells were imaged in each condition ($n = 900$). For vRNA detection, 100 cells were imaged for each condition ($n = 100$). Except for HIV-, 37 cells were imaged for vDNA and vRNA detection. Results from 1 representative experiment out of 2 are shown. Source data are provided in the source data file. NC, negative control; vDNA, viral DNA; vRNA, viral RNA.

software[56] indicate that CX014442 and ZL0580 work additively in silencing HIV-1 gene expression in non-reactivated cells (Fig. 5b). After reactivation with TNF-α, ZL0580 dose-dependently blocked HIV-1 reactivation in cells with and without treatment with CX014442 (± 90% inhibition at 10 μM ZL0580) (Fig. 5c). Synergy calculations revealed here as well additive effects of ZL0580 and CX014442 and almost a complete block of HIV-1 reactivation after administration of a high concentration of both compounds (Fig. 5d).

Persistence of BRD4 modulators after CX014442 treatment in SupT1 cells

Next, we verified the persistence of the both JQ1 and ZL0580 on CX014442-retargeted SupT1 cells according to the protocol described in the methods section and presented in Fig. S10a. First, we tested the persistent effect of JQ1 on CX014442-retargeted proviruses in non-reactivated cells. In line with the results of Fig. S4b, JQ1 dose-dependently promoted basal transcription 48 h after its drug removal, independent of CX014442 treatment (Fig. S10b). However, in the presence of TNF-α, no promotion persisted after JQ1 removal, both with and without CX014442-treatment (Fig. S10c). Similar experiments were performed in the presence of ZL0580. Although ZL0580 dose-dependently decreased basal transcription and reactivation of CX014442-retargeted proviruses on day 11 post-transduction, this effect did not persist, both in non-reactivated and reactivated cells (Fig. S10d, e). Altogether, these results show that the stimulatory effect of JQ1 on LEDGF/p75-dependent and CX014442-retargeted proviruses is preserved for 48 h after withdrawal from cell culture. With respect to ZL0580, the inhibitory effects did not persist, nor in LEDGF/p75-dependent provirus nor in CX014442-retargeted provirus.

ZL0580 inhibits HIV-1 transcription in primary cells

Next, the impact of ZL0580 on HIV-1 transcription was investigated in more clinically relevant cells, namely human PBMCs. PBMCs were extracted from buffy coats of 4 healthy donors. PBMCs were stimulated with 10 μg/mL phytohemagglutinin (PHA) to enhance infection susceptibility. 3 days after infection, residual virus was washed away. ZL0580 was added on day 7 and samples were harvested 24 h after treatment for the luciferase assay. To assess whether ZL0580 silenced HIV-1 transcription after its removal, the compound was washed away on day 8 and the cells were cultured for 3 days while following up the luciferase reporter expression (Fig. 6a). On day 8, ZL0580 dose-dependently reduced LTR-driven luciferase activity in donor 1 ($IC_{50} = 10.28 \pm 0.47$ μM) (Fig. 6b; Table S4). In subsequent donors, we assessed the persistence of the inhibitory effect of ZL0580 by harvesting samples after ZL0580 removal (days 9-11). In donor 2, ZL0580 dose-dependently reduced HIV-1 transcription on day 8 post-transduction ($IC_{50} = 10.68 \pm 1.51$ μM). The effect persisted modestly 24 h after compound removal (day 9) but gradually diminished over time the next days (days 10 and 11) (Fig. 6c). Donor 3 significantly maintained inhibition of HIV-1 transcription for 24 h after compound removal (day 9), but the effect was lost as well by day 10 (Fig. 6d). Propidium iodide staining indicated that ZL0580 only markedly reduced cell viability at 15 μM (Fig. 6e). Donor 4 also maintained inhibition for 24 h after treatment interruption, with only modest cell viability loss at 15 μM (Fig. 6f, g). Table S4 shows the IC_{50} calculated for each donor on day 8 post-transduction, resulting in an average IC_{50} of 11.09 ± 1.55 μM. For donors 3 and 4, the CC_{50} was not reached in the concentrations tested. To calculate the exact CC_{50} with flow cytometry, PBMCs of donor 3, 4, and 5 were incubated with ZL0580 for 24 h. Across these donors an average CC_{50} of 20.68 ± 3.34 μM was calculated (Fig. S11a). In addition, the more sensitive MTT assay was used to determine toxicity of ZL0580 in PBMCs. PBMCs were treated with ZL0580 according to Fig. 6a and on day 8 post-transduction the MTT assay was performed. Across donor 1, 4, and 8 an average CC_{50} of 13.50 ± 0.94 μM was calculated (Fig. S11b). Table S4 summarizes the IC_{50} and CC_{50}, with both flow cytometry and the MTT assay, across all donors. An average SI was determined of 1.89 ± 0.42 after using flow cytometry and 1.22 ± 0.19 after using the MTT assay (Table S4). Although, in PBMCs, ZL0580 exhibited slightly lower toxicity compared to SupT1 and J-Lat A2 cells, the compound's active concentration range remains close to its toxic threshold. To further evaluate this, we overlaid the LPA activity data (measured via the luciferase reporter assay) with toxicity data (measured using propidium iodide staining and/or the MTT assay). In donors 3 and 4, this analysis confirmed that the effect of ZL0580 is HIV-specific, as particularly at concentrations below 10 μM, the reduction in luciferase reporter expression (LPA activity) was more pronounced than the decline in cell viability (Figs. S11c, d). Furthermore, flow cytometry and MTT assays indicated no significant toxicity at concentrations below 6.25 μM (flow cytometry; Fig. S11a) and 10 μM (MTT assay; Fig. S11b). Importantly, at these non-toxic concentrations, HIV-1 transcription inhibition was already observed, further supporting the conclusion that the effect of ZL0580 is specific to HIV-1 transcription. Altogether, these results collectively suggest that ZL0580 silences HIV-1 transcription in primary cells, but that the effect is only maintained for a short period of time after compound removal.

The effect of ZL0580 in primary cells after multiple treatments

Next, we investigated whether multiple treatments could extend the duration of the persistent effect. First, cells were treated with ZL0580 for 24 h twice, according to the protocol outlined in Fig. 7a. Briefly, cells were infected with HIV-1 FLuc virus and treated with ZL0580 2 times for 24 h between days 5 and 8 post-transduction. Persistence of the LPA activity was evaluated 1 to 3 days after ZL0580 removal. In donor 3 and 7, LTR-driven luciferase reporter expression was reduced dose-dependently on day 8 (Fig. 7a). While the magnitude of the inhibitory effect after two ZL0580 treatments was not exceeding those after a single treatment (Fig. 6), the persistence of the LPA activity was markedly longer. In Fig. 6d, the LPA activity of ZL0580 completely disappeared starting from day 10. However, after double treatment with ZL0580, HIV-1 transcription modestly remained suppressed 3 days after treatment-interruption (Fig. 7a). To assess toxicity after double treatment, cell viability was evaluated on day 8 post-transduction using propidium iodide staining and flow cytometry.

https://doi.org/10.1038/s41467-025-59398-7

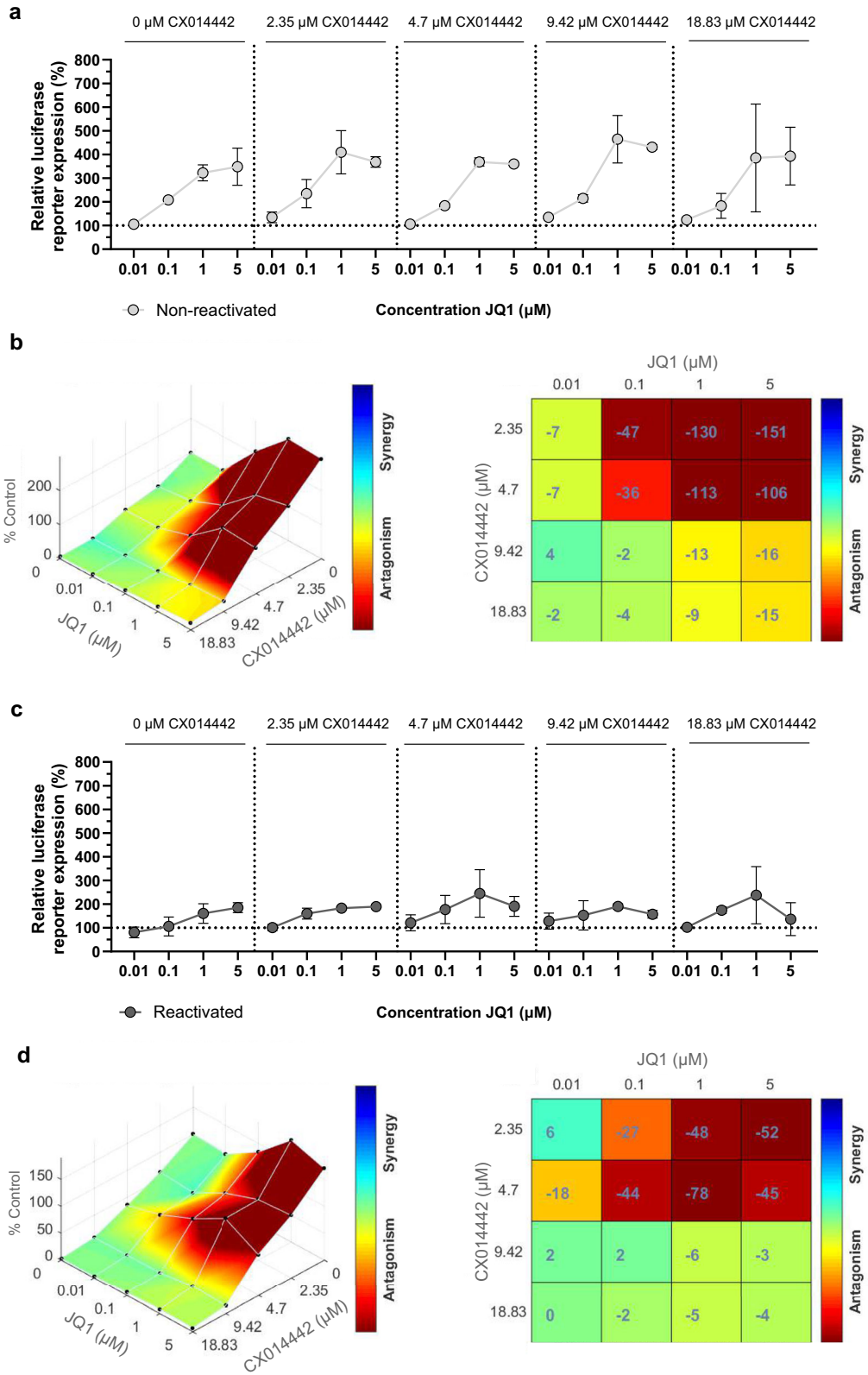

Multiple treatments did not increase ZL0580's toxicity in primary cells compared to single treatment (Fig. 7c). However, a major limitation of this experiment is that toxicity was only measured on day 8 post-transduction, leaving uncertainty about potential effects on cell viability at days 9 to 11 post-transduction. Moreover, toxicity was assessed with propidium iodide instead of the more sensitive MTT assay. The modest inhibition of HIV-1 transcription observed in donor 3 at 2.5–5 μM ZL0580 may correspond to the modest reduction in cell viability detected at day 8. At 10 and 15 μM, the inhibition of HIV-1 transcription was more pronounced (Fig. 7a) compared to the reduction in cell viability (Fig. 7c) in this experiment. However, given the substantial cytotoxicity observed at 15 μM in Fig. 6e and because propidium iodide staining was used instead of the MTT assay, it remains uncertain whether the persistent transcriptional inhibition is

Fig. 4 | JQ1 shows less antagonism after LEDGIN CX014442 treatment. a, c The luciferase counts, obtained by the luciferase assay on day 11 following Fig. 3b were normalized for the total concentration of protein (determined with BCA assay). The relative luciferase reporter expression (%) was calculated by dividing the luciferase counts normalized for protein content (BCA assay) from the JQ1-treated cells by those from the control (0 µM JQ1). This was calculated separately for each concentration of CX014442 and for non-reactivated (light grey) **(a)** and reactivated cells (dark grey) **(c)**. Mean ± SD of 2 representative experiments out of 5 are shown ($n = 2$). **b, d** Using the Combenefit software, experimental 3D dose-response curves of the drug combination of CX014442 and JQ1 were generated, expressed as a percentage of the positive control (0 µM CX014442 and JQ1). The curve is covered with a color code according to synergy/antagonism scores, calculated with the Bliss Synergy model. A red color indicates antagonism, a green color additivity and a blue color synergism. The matrix shows the value of the synergy/antagonism scores. A synergy score below -10 indicates antagonism, a synergy scores between -10 and 10 indicates additivity and a synergy score higher than 10 indicates synergy. This is shown for both the non-reactivated **(b)** and the TNF-α reactivated cells **(d)**. The average results from 2 biological duplicates of 1 representative experiment out of 5 are shown ($n = 2$). Figures are created with Combenefit[56]. Statistics were not performed due to limited number of datapoints. Source data are provided in the source data file. BCA, bicinchoninic acid; ns, non-significant; TNF-α, tumor necrosis factor α; 3D, 3-dimensional.

solely due to LPA activity or if cytotoxic effects also contribute at this concentration. In donor 7, overall less toxicity of ZL0580 was observed at day 8, indicating that the reduction in luciferase expression is not solely attributable to cytotoxicity (Fig. 7c).

Next, cells were treated 3 times with ZL0580 for 24 h between days 3 and 8 post-transduction (Fig. 7b). The magnitude of the effect again remained comparable to that observed after one or two treatments (Fig. 7b). Donor 3 exhibited persistence for one day (until day 9), while donor 7 showed persistence for two days (until day 10) (Fig. 7b). An unexpected increase in luciferase expression was observed in donor 3 on days 10 and 11 post-transduction, but this effect displayed high variability. It remains unclear whether this increase is due to a technical artifact or caused by cytotoxicity. Since cell viability was only assessed on day 8 post-transduction using propidium iodide staining, potential viability effects at later time points cannot be ruled out (Fig. 7c).

In conclusion, multiple treatments extend the duration of ZL0580's LPA activity, with two treatments yielding more favorable results than three. The reason for this trend remains unclear and requires further investigation. While ZL0580 shows promise for sustained HIV-1 transcriptional inhibition after multiple treatments in donor 7, its effects at higher concentrations may be influenced by cytotoxicity in donor 3. Further studies are needed to differentiate between specific transcriptional suppression and potential cell viability effects after multiple treatments, as toxicity may vary between donors. In the future such repeated treatments could be done using the more specific compound 24.

LEDGIN CX014442 and ZL0580 additively inhibit HIV-1 transcription in primary cells

Next, we tested the combination of the LPAs ZL0580 and CX014442 in primary cells. First, the IC_{50} of a new batch of CX014442 was determined in PBMCs from donor 5 at 20.87 ± 2.54 µM (Fig. 8a). Concentrations ranging from 10.44-41.74 µM (0.5-2 x IC_{50}) were used. Toxicity assessment showed that CX014442 did not affect the cell viability in PBMCs at the concentrations used (Fig. 8b). Next, the LEDGIN CX014442 was combined with ZL0580, according to the protocol described in Fig. 8c. Results from one donor (donor 3) are shown in Fig. 8d, e and results from 3 other donors (donor 2, donor 4, and donor 6) are shown in Fig. S12. The luciferase counts of the ZL0580-treated wells were normalized to the control condition without ZL0580-treatment for each concentration of CX014442 to compare the effect of ZL0580 on LEDGF/p75-targeted *vs.* LEDGIN-retargeted provirus. In donor 3, a ± 75% decrease in luciferase reporter expression was observed at the highest concentration of ZL0580 (15 µM) compared to the control condition without ZL0580-treatment, independent of CX014442 treatment (Fig. 8d). Next, the Combenefit software was used to model the luciferase activity in a 3D graph and to calculate the synergy scores based on the bliss model[56]. This analysis revealed that a combined treatment of ZL0580 and CX014442 reduced HIV-1 transcription even more potently compared to a single treatment with one of the two LPAs (Fig. 8e). In accordance, synergy calculations indicated that CX014442 and ZL0580 work additively in silencing HIV-1 transcription (Fig. 8e). In donor 4, ZL0580 reduced HIV-1 transcription significantly (± 60%), also independent of CX014442-treatment. In line, additive synergy scores were calculated (Fig. S12a). In donor 2 and 6, ZL0580 reduced basal HIV-1 transcription independent of CX014442 treatment, although to a lesser extent compared to other donors tested. After treatment with 41.74 µM CX014442, data were skewed and ZL0580 did not dose-dependently decrease HIV-1 transcription (Fig. S12b; S12c). Overall, while there was some donor-dependent variation, combined treatment with CX014442 and ZL0580 additively blocked HIV-1 transcription, achieving near-complete silencing at high concentrations of both.

Finally, we studied the persistence of the combined treatment of LEDGIN and ZL0580 in primary cells. Experiments have been performed as described in the methods section and as illustrated in Fig. S13a. The experiment was conducted with 2 donors. Both in donor 3 and 4 on day 8 post-transduction, ZL0580 reduced basal HIV-1 transcription to the same extent, independent of CX014442 treatment (Fig. S13b, S13c). Without CX014442 treatment or after addition of low concentrations of CX014442 (10.44 µM), the inhibitory effect of ZL0580 on basal transcription persisted for one day after compound removal (until day 9). Interestingly, at higher concentrations of CX014442 (20.87-41.74 µM), ZL0580's effect persisted for 2 days after compound removal (until day 10). Unfortunately, the effect was lost 3 days after compound removal (day 11) (Fig. S13b, S13c). To conclude, these results indicate that the inhibitory effect of ZL0580 on HIV-1 transcription persists slightly longer on LEDGIN-retargeted proviruses compared to LEDGF/p75-dependent provirus in primary cells.

Discussion

HIV-1 remains incurable due to the persistence of a latent reservoir. The "block-and-lock" strategy aims to silence this reservoir by using LPAs to block HIV-1 transcription and lock the provirus in a deep latent state. BRD4, which negatively regulates HIV transcription, can be modulated by small molecules like JQ1 to enhance transcription[46–50,52,57,58], while ZL0580 paradoxically silences HIV expression in various cell types[51,53]. This study compares JQ1 and ZL0580 to explore BRD4's role in HIV-1 transcription. Our luciferase assay corroborates that JQ1 promotes HIV-1 transcription with an optimum at 1 µM (Fig. 1c, d). Most studies reported a dose-dependent effect of JQ1, while Bartholomeeusen et al. also observed a maximum stimulation of HIV-1 transcription at 5 µM of JQ1[47]. This optimal concentration may mean that JQ1 reaches a maximum effect around this concentration. However, the slight decrease in relative luciferase reporter expression from 1-5 µM may also point towards a more complex role of BRD4 in HIV-1 transcription. Initial research claimed that BRD4 activates HIV-1 transcription by recruiting P-TEFb to RNA polymerase II (Fig. 9a**; model 2)**[59–63]. However, subsequent studies highlighted BRD4's role as a repressor of HIV-1 transcription by competing with Tat for P-TEFb binding (Fig. 9a**; model 1)**[46–48,50]. Others observed that the BRD4 short isoform (BRD4S) recruits the BAF chromatin remodeling complex to the HIV promotor, further blocking HIV-1 transcription independently of Tat (Fig. 9a**; model 3)**[64]. Additionally, BRD4 may enhance

https://doi.org/10.1038/s41467-025-59398-7

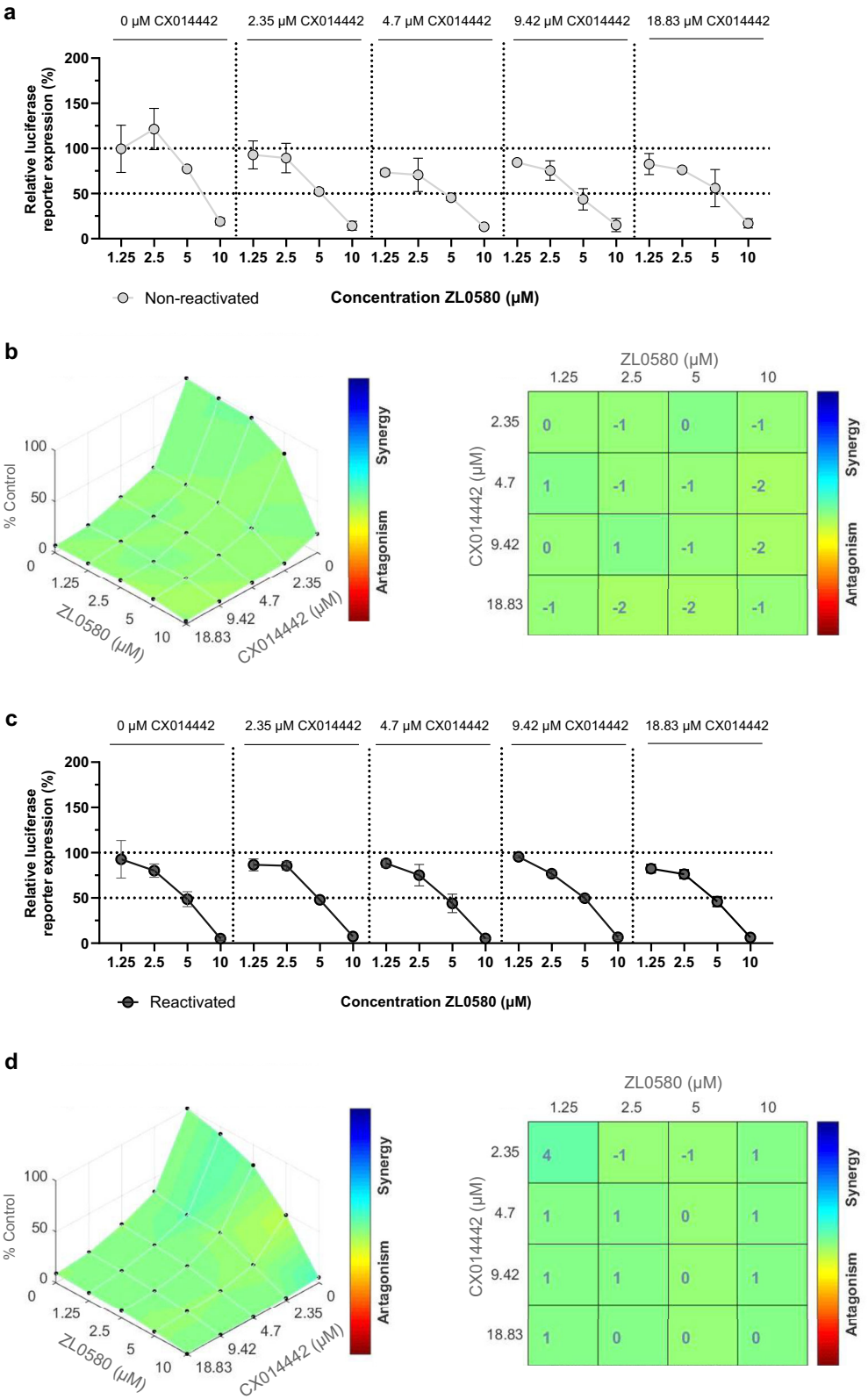

transcription via enhancer-mediated mechanisms (Fig. 9a**; model 4)**[45,65]. The bimodal effect of JQ1 on HIV-1 transcription may be the result of an interplay between these mechanisms. At low concentrations of JQ1 (<1 µM), JQ1 could reactivate HIV-1 transcription with model 1 and 3 (Fig. 9a). At higher concentrations (>1 µM), JQ1 could block HIV-1 transcription through model 2 and 4 (Fig. 9a). In addition, our result indicate that the effect of JQ1 on basal transcription is more pronounced than the effect on TNF-α mediated reactivation (Fig. 1c, d). Literature indeed shows that JQ1 suppresses TNF-α mediated NF-kB transcription[66–68]. A second hypothesis is that 10 ng/mL TNF-α reaches a maximum level of stimulation, which could not be further enhanced by JQ1. To test this hypothesis, lower concentrations of TNF-α could be administered together with JQ1.

Fig. 5 | ZL0580 shows additive effects with LEDGIN CX014442 in inhibiting HIV-1 transcription and reactivation. a, c The luciferase counts, obtained by the luciferase assay on day 11 following Fig. 3b, were normalized for the total concentration of protein (determined with BCA assay). The relative luciferase reporter expression (%) was calculated by dividing the luciferase counts normalized for protein content (BCA assay) from the ZL0580-treated cells by those from the control (0 µM ZL0580). This was calculated separately for each concentration of CX014442 and for non-reactivated (light grey) **(a)** and reactivated cells (dark grey) **(b)**. Mean ± SD of 2 biological duplicates of 1 representative experiment out of 7 are shown ($n = 2$). **b, d** Using the Combenefit software, experimental 3D dose-response curves of the drug combination of CX014442 and ZL0580 were generated, expressed as a percentage of the control (0 µM CX014442 and ZL0580). The curve is covered with a color code according to synergy/antagonism scores, calculated with the Bliss Synergy model. The matrix shows the value of the synergy/antagonism scores. A synergy score below -10 indicates antagonism, a synergy scores between -10 and 10 indicates additivity and a synergy score higher than 10 indicates synergy. This is shown for both the non-reactivated **(b)** and the TNF-α reactivated cells **(d)**. The average results from 2 biological duplicates of 1 representative experiment out of 7 are shown ($n = 2$). Statistics were not performed due to limited number of datapoints. Figures are created with Combenefit[56]. Source data are provided in the source data file. BCA, bicinchoninic acid; ns, non-significant; TNF-α, tumor necrosis factor α; 3D, 3-dimensional.

The mechanisms whereby JQ1 affects HIV-1 transcription have been extensively investigated. Paradoxically, ZL0580 has only been investigated by one group, which discovered its LPA activity (IC_{50} = ~ 8 µM in J-Lat cells; ~ 2.5 µM in $CD4^+$ T cells)[51–53]. We confirmed that ZL0580 dose-dependently reduces HIV-1 transcription, in SupT1 cells (Fig. 1e, f), J-Lat A2 cells (Fig. S3a) and PBMCs (Fig. 6). Table S4 summarizes ZL0580's activity and toxicity across different cell lines. A major concern remains the high toxicity as,ociated with ZL0580. A relatively low SI of 1.77 ± 0.13 (non-reactivated) and 2.63 ± 0.26 (reactivated) was calculated in SupT1 cells using propidium iodide staining to determine the CC_{50}. With the MTT assay, the SI was calculated at 1.10 ± 0.08 (non-reactivated) and 2.06 ± 0.21 (reactivated). Due to the low SI in non-reactivated cells, we cannot fully exclude the possibility that the LPA activity of ZL0580 is partially influenced by its cytotoxicity. However, several lines of evidence suggest that the observed reduction in HIV reactivation is not solely attributable to toxicity. First, the decrease in luciferase expression is more pronounced than the reduction in cell viability (Fig. 1f and S1b–f). Second, even at lower concentrations where cytotoxicity is minimal, a substantial decrease in HIV transcription levels is still observed (Fig. 1f and S1b–f). Third, the ZL0580 analogue, compound 24, exhibits no detectable cytotoxicity while maintaining LPA activity (Fig. S2). Fourth, ZL0580 blocked Tat-dependent transcription in HeLa-TZMbl cells without its associated toxicity (Fig. 2g). Nonetheless, a limitation of our study is that cytotoxicity was not consistently assessed using the MTT assay; in some instances, we relied on propidium iodide staining only, which detects only late-stage cell death based on membrane integrity and does not capture early cytotoxic effects or cellular stress responses. In PBMCs, a more clinically relevant model, ZL0580 exhibits slightly lower toxicity but also reduced LPA activity compared to SupT1 cells, with variability between donors (Fig. 6 and S11). On average, the selectivity index (SI) was calculated as 1.89 ± 0.42 when toxicity was assessed using propidium iodide and 1.22 ± 0.19 when the CC_{50} was determined with the MTT assay (Table S4). The reduced toxicity in PBMCs compared to cancer cell line models may relate to BRD4's critical role in cancer biology[66–68]. Still the SI of ZL0580 is relatively low. Notably, ZL0580 effectively suppressed HIV-1 transcription at non-toxic concentrations, at or below 10 µM (MTT; Fig. S11b) or 6.25 µM (flow cytometry; Fig. S11a), indicating that its LPA effect is specific to HIV transcription. To further evaluate this, we superimposed the LPA activity data (measured via the luciferase reporter assay) with toxicity data (measured using propidium iodide staining and/or the MTT assay). This overlay demonstrated as well that the reduction in luciferase reporter expression was significantly more pronounced than the reduction in cell viability, particularly at concentrations below 10 µM (Fig. S11c, d). These findings reinforce the HIV-specific activity of ZL0580, while also highlighting the need for further optimization to reduce toxicity and enhance its therapeutic window. Preliminary studies on the ZL0580 analogue, compound 24, suggest that it is possible to maintain the LPA activity of ZL0580 while reducing cytotoxicity (Fig. S2). However, further investigation is required to fully evaluate the potential of compound 24 within the block-and-lock cure strategy and to develop more promising ZL0580 analogues.

Next, mechanistic differences in BRD4 modulation by JQ1 and ZL0580 were investigated. Binding assays and docking analyses by the Hu group showed that unlike the pan-inhibitor JQ1, ZL0580 selectively binds to BRD4 over other members of the BET family[51–53]. In addition, ZL0580 shows higher affinity for bromodomain (BD) 1 compared to BD2[51–53]. While JQ1 binds to the KAc binding pocket of BET proteins[55], ZL0580 is thought to bind a distinct non-KAc site[51–53]. Co-IPs and ChIP-seqs corroborated that JQ1 and ZL0580 induced opposite protein-protein and protein-chromatin interactions during Tat-dependent transcription[51–53]. To further explore their mechanisms, we applied bDNA imaging, which visualizes HIV-1 proviral DNA and RNA transcripts simultaneously at single-cell level. These experiments confirmed that both JQ1 and ZL0580 work on the transcriptional level (Fig. 2a–d; S6; S7), more specifically Tat-dependent transcription (Fig. 2g). Future studies should explore if these compounds interfere in other steps of HIV-1 transcription (initiation, elongation, termination), as explored by the Yukl lab[69]. Additionally, we assessed BRD4 co-localization with acetylated histones in the presence of both compounds and found that JQ1 decreases and ZL0580 increases BRD4 binding to acetylated histones (Fig. 2e, f). This suggest as well that ZL0580 binds to a non-lysine binding pocket of BRD4, as BRD4 is not displaced from the acetylated histone. However, to define the exact molecular interaction patterns of ZL0580 and BRD4, co-crystal structures are warranted.

A perfect LPA should epigenetically silence the HIV promotor, as HIV-1 gene expression needs to be suppressed when therapy is absent. Therefore, we determined whether the effect of JQ1/ZL0580 persisted after compound removal. The effect of JQ1 on basal transcription persisted in SupT1 cells (Fig. S4b), possibly due to the induction of a permissive chromatin structure by alterations in the recruitment of chromatin remodeling complexes[51,64]. The effect of JQ1 on TNF-α reactivated cells did not persist (Fig. S4c). This may arise from direct interactions of JQ1 or TNF-α counteracting JQ1's epigenetic effects[70,71]. Alternatively, TNF-α reached a maximum stimulation at 10 ng/mL that cannot be further enhanced by JQ1. In SupT1 cells, the LPA effect of ZL0580 did not persist after compound removal (Fig. S5). In PBMCs, the LPA activity of ZL0580 was maintained for only one day post-removal, without affecting cell viability (Fig. 6). Interestingly, multiple treatments significantly extended the duration of the persistent effect up to 3 days (Fig. 7). However, further studies are required to assess the potential contribution of ZL0580-induced cytotoxicity to this effect. Persistence of ZL0580's effect may depend on (i) the fraction of BRD4 occupied by ZL0580, which could be increased after multiple treatments; (ii) selective killing of infected cells by ZL0580; (iii) epigenetic reprogramming of the HIV promotor by ZL0580. Multiple treatments may result in a cumulative and more stable alteration of the chromatin structure, extending the duration of the effect. Evidence from the Hu group previously suggested that ZL0580 reprograms the HIV promotor epigenetically. First, ZL0580 was able to silence HIV-1 gene expression in resting PBMCs, harboring low levels of Tat[51]. Second, single dosing with ZL0580 rendered J-Lat cells resistant to reactivation for 14 days and microglial cells for 21 days[51–53]. Third, MNAse

https://doi.org/10.1038/s41467-025-59398-7

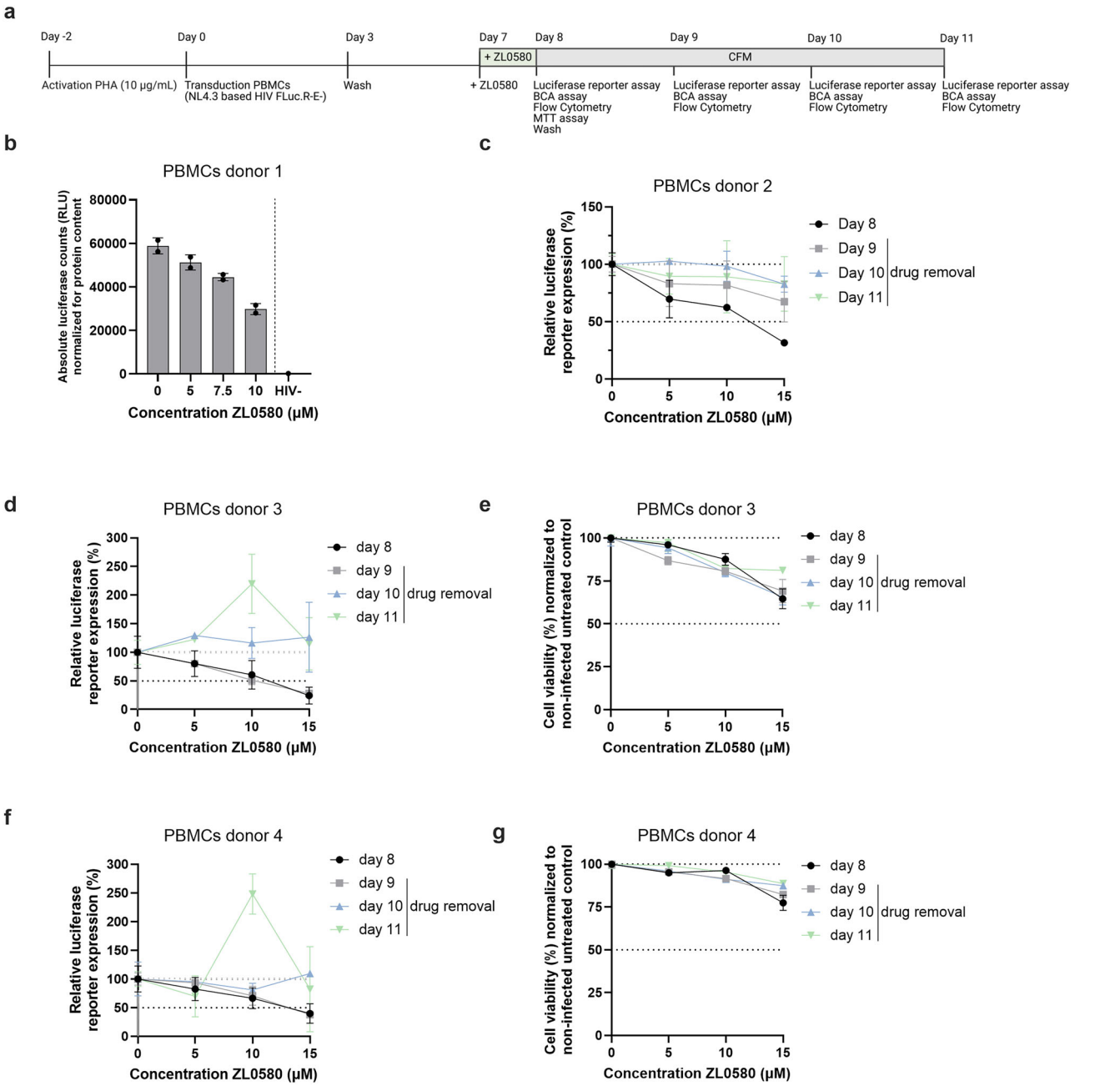

Fig. 6 | ZL0580 inhibits HIV-1 transcription in primary cells. a PBMCs were stimulated with 10 µg/mL PHA for 2 days. The cells were transduced with HIV-1 FLuc virus. After 3 days, residual virus was washed away. 7 days post-transduction, ZL0580 was added to the wells. 24 h later, samples were harvested to perform luciferase assays and flow cytometry. Cells were washed and subcultured. CFM indicates compound free media. 1, 2 and 3 days after drug removal, samples were harvested for luciferase assays and flow cytometry. **b** For donor 1, luciferase counts are presented for the cells harvested on day 8 post-transduction. Luciferase counts were normalized for the total concentration of protein (determined with BCA assay). HIV- are the non-transduced cells (negative control). Each dot represents one biological duplicate. Mean ± SD of biological duplicates are shown ($n = 2$). **c, d, f** For donor 2 **(c)**, donor 3 **(d)** and donor 4 **(f)**, relative luciferase reporter expression (%) was calculated by dividing the luciferase counts normalized for protein content (BCA assay) from ZL0580-treated cells by those from the control (0 µM ZL0580). Results from samples harvested on day 8 (black dot), 9 (grey square), 10 (blue triangle) and 11 (green reversed triangle) are presented. Mean ± SD of biological duplicates are shown for each donor ($n = 2$; 4 donors). **e, g** For donor 3 **(e)** and donor 4 **(g)**, cell viability was determined in parallel by staining with propidium iodide and flow cytometric analysis. The cell viability was normalized to the non-infected untreated control. Mean ± SD of biological duplicates from each donor are shown ($n = 2$; 2 donors). Statistics were not performed due to a limited number of data points. Source data are provided in the source data file. BCA, bicinchoninic acid; CFM, compound free media; HIV-, non-transduced negative control; IC_{50}, 50% inhibitory concentration; ns, non-significant; PBMCs, peripheral blood mononuclear cells; PHA, phytohemagglutinin; RLU, relative light units.

nucleosomal mapping indicated that ZL0580 (10 µM) induces a repressive chromatin structure at the HIV LTR[51]. All these observations point towards ZL0580-induced epigenetic reprogramming of the LTR. However, this reprogramming may be cell-type specific, as its persistence was longer in microglial cells[51–53] compared to PBMCs. Future studies should explore ZL0580 analogues with a more favorable SI to further investigate this epigenetic programming.

An important hurdle for the block-and-lock cure strategy is the heterogeneous identity of the latent reservoir, which is partially driven by the diversity in integration site selection. Therefore, combinations

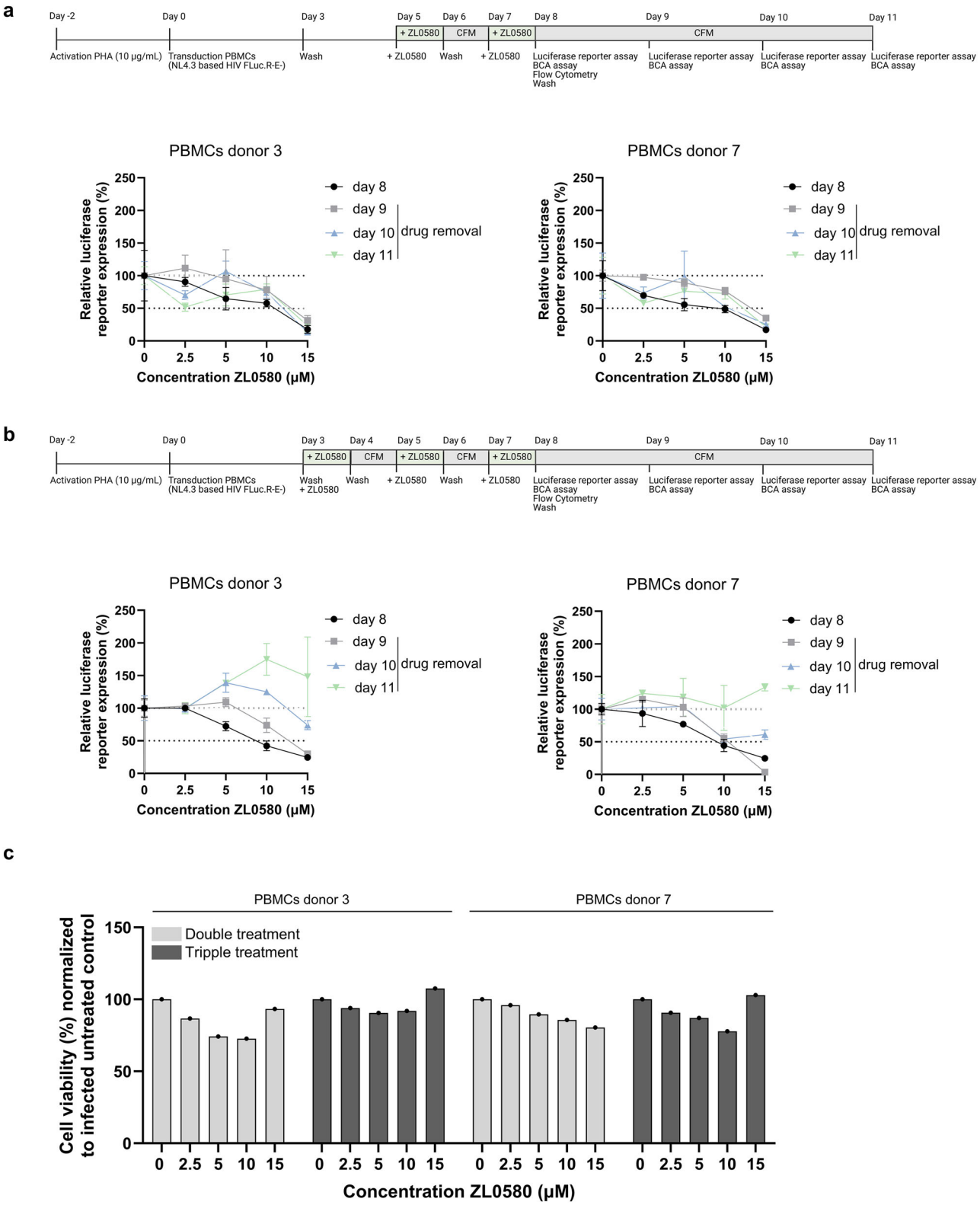

of LPAs that silence proviruses at distinct integration sites are warranted. LEDGINs are well-characterized LPAs that inhibit integration and retarget the residual provirus to transcriptionally silent genes (Fig. 9b)[35–40]. Unfortunately, previous single-cell experiments indicated that residual viral expression persisted in some cells even after high doses of LEDGINs[41]. Chen et al found a positive correlation between the proximity of integration sites to enhancers and HIV-1 gene expression[72]. Vansant et alshowed that LEDGINs do not influence the proximity of integration sites to enhancers. Moreover, the authors showed that the cells containing high vRNA expression after LEDGIN treatment were integrated in proximity to enhancer sites[41]. It remains unknown whether the integration near enhancer sites occurs randomly or whether it is the nature of the virus to do so. Moreover, since integration near enhancers is LEDGF/p75-independent, it is uncertain if

Fig. 7 | The effect of ZL0580 in primary cells after multiple treatments. a, b PBMCs were stimulated with 10 µg/mL PHA for 2 days. The cells were transduced with HIV-1 FLuc virus. After 3 days, residual virus was washed away. Between day 3 and 7 post-transduction, cells were pretreated twice **(a)** or thrice **(b)** with ZL0580 for 24 h. CFM indicates compound free media. After the final ZL0580-treatment (day 8 post-transduction), samples were harvested to perform luciferase assays and flow cytometry. To determine if the effect of ZL0580 persisted after ZL0580 removal, cells were washed and subcultured. 1, 2 and 3 days after drug removal, samples were harvested for luciferase assays. Luciferase counts were normalized for the total concentration of protein (determined with BCA assay). Relative luciferase reporter expression (%) was calculated by dividing the luciferase counts normalized for protein content (BCA assay) from ZL0580-treated cells by those from the control (0 µM ZL0580). Results from samples harvested on day 8 (black dot), 9 (grey square), 10 (blue triangle) and 11 (green reversed triangle) are presented. Mean ± SD of technical duplicates from each donor are shown ($n = 2$; 2 donors). **c** Cell viability was determined in parallel with the luciferase assay on day 8 post-transduction by staining with propidium iodide and flow cytometric analysis. The cell viability of the ZL0580-treated wells was normalized to the infected untreated control. The value of one technical duplicate from each donor is shown ($n = 1$; 2 donors). Statistics were not performed due to a limited number of data points. Source data are provided in the source data file. BCA, bicinchoninic acid; CFM, compound free media; ns, non-significant; PBMCs, peripheral blood mononuclear cells; PHA, phytohemagglutinin; RLU, relative light units.

the high vRNA expressing cells are treated with LEDGINs or escaped LEDGIN-treatment (Fig. 9b)[41]. Either way, combining LEDGINs with enhancer antagonist (BRD4 modulators) may completely silence HIV-1 gene expression, making such combinations a promising strategy for the block-and-lock functional cure (Fig. 9b). Lovén et al. reported that JQ1 decreased the expression of enhancer-related genes and even decreased the level of BRD4 at the genomic enhancer regions[45]. However, JQ1 also reactivates HIV-1 transcription, making ZL0580, a BRD4 modulator which epigenetically represses HIV-1 transcription, a more promising compound for combination with LEDGINs. However, since ZL0580 is newly discovered, its specific effects on the enhancer biology are still unknown. Because ZL0580 alters BRD4's interaction profile with proteins and the chromatin differently than JQ1, its effectiveness in blocking enhancer-dependent transcription remains unclear. Thus, we combined LEDGINs with both JQ1 and ZL0580 to more efficiently block HIV-1 gene expression.

Synergy calculations using Combenefit[56], corroborated that JQ1 acts differently on LEDGIN-retargeted proviruses in SupT1 cells (Fig. 4). The switch towards less antagonistic synergy scores at higher LEDGIN concentrations suggest that JQ1 may block enhancer-dependent transcription after LEDGIN-mediated retargeting. However, since JQ1 acts predominantly as a LRA, it was not capable to silence residual HIV-1 transcription (Fig. 4). Next, we combined CX014442 and ZL0580, both in cell line models (Fig. 5) and PBMCs (Fig. 8; S12). Interestingly, our Combenefit analysis confirmed an additive effect between these 2 agents and almost a complete block of the luciferase expression at high concentrations of both agents (Figs. 5 and 8, S12). In addition, we tested whether treatment with CX014442 affected the persistence of the inhibitory effect of ZL0580 on HIV-1 transcription. Interestingly, in PBMCs the inhibitory effect of ZL0580 on HIV-1 transcription persisted longer in cells treated with high concentrations of CX014442 compared to cells not treated or treated with lower concentrations of CX014442 (1 *vs.* 2 days) (Fig. S13). This may indicate that integration sites influence the epigenetic modifications ZL0580 imparts to the chromatin. In addition, it may also be possible that when HIV-1 is integrated into silent regions, the transcriptional activity of the provirus is already reduced significantly, making it more challenging for viral gene expression to be reactivated. Altogether, we showed that the combination of ZL0580 with CX014442 nearly achieved complete silencing of HIV-1 gene expression. While direct evidence for our enhancer hypothesis is lacking, ZL0580 and LEDGINs still show promise as an 'LPA cocktail' candidate for a block-and-lock cure. Furthermore, this highlights as well that combining different LPAs in a rational could be crucial for achieving a more effective block-and-lock cure strategy. More combinations should be investigated using synergy calculations, such as with didehydrocortistatin A[19,20].

While ZL0580 requires more optimization regarding toxicity, potency, and persistence before being included in animal studies and clinical trials, BRD4 modulators offer several key advantages. First, viral resistance is ruled out because BRD4 is a host protein. Second, BRD4-targeting compounds have shown promising safety profiles in oncology trials[73–75]. Third, ZL0580 can repress HIV-1 replication in microglial cells and macrophages, which are insufficiently targeted by ART[76]. Fourth, BRD4 modulators target transcriptional events after viral integration, while LEDGINs target HIV-1 integration. Therefore, LEDGINs were administered during acute infection in our model, while ZL0580 was added after the induction of latency during chronic infection. Studies showing that the replication-competent reservoir is established around the time of therapy initiation[77,78], suggest that LEDGINs can alter the HIV-1 integration site in chronically infected patients diagnosed years after infection as well. The challenge is whether LEDGINs can modulate the latent reservoirs after treatment interruption in chronically infected patients already treated with cART. Further research into the effectiveness of LEDGINs on the established latent provirus (discussed in ref. 4,79) is still warranted.

To conclude, our data confirm that BRD4 can be modulated to either stimulate or hamper HIV-1 transcription. Furthermore, ZL0580 shows promise in combination with LEDGINs to reinforce the block-and-lock cure strategy. Still, ZL0580 requires further mechanistic investigation and lead optimization to reduce toxicity and optimize the persistence of the LPA effect.

Methods

Cell culture

SupT1 cells (T lymphoblasts, ARP-100)[80] (acquired through the National Institutes of Health (NIH) AIDS reagent program, Bethesda, MD) were cultured in Roswell Park Memorial Institute (RPMI) medium (GIBCO) in the presence of 10% (v/v) fetal bovine serum (FBS; GIBCO) and 0.01% (v/v) gentamicin (GIBCO). J-LatA2 cells(T lymphoblasts; ARP-9854)[81] (acquired through the HIH AIDS reagent program, Bethesda, MD) were cultured in RPMI medium (GIBCO) in the presence of 10% (v/v) FBS (GIBCO), 0.01% (v/v) gentamicin (GIBCO) and 1% (v/v) glutamax (GIBCO). HeLa-derived TZM-bl cells[82] (cervical carcinoma; ARP-8129)[83] (acquired through the NIH AIDS reagent program, Bethesda, MD) were cultured in Dulbecco modified Eagle medium (DMEM; GIBCO) with 10% (v/v) FBS (GIBCO), 0.01% (v/v) gentamicin (GIBCO). Cells were cultured at 37 °C in a humidified atmosphere of 5% CO_2. All cells were verified to be free from mycoplasma contamination each month (PlasmoTest™, InvivoGen Europe).

Virus strain. The pNL4-3.Luc.R-E-based HIV-1 construct, which contains a firefly luciferase gene in the pNL4.3 *nef* gene and 2 frameshifts (5' Env and Vpr aa 26), was obtained through the NIH AIDS Research and Reagent Reference program[84]. HEK-293T cells were co-transfected with pNL4-3.Luc.RE- and pVSV-g to produce replication-deficient (single-round) virus encoding luciferase, as previously described[30,85,86]. We further refer to this virus as HIV-1 FLuc virus.

Compounds

The BRD4 inhibitor, JQ1, was obtained from Sigma Aldrich. ZL0580 was a kind gift from Dr. Peng (Shandong University). Cistim/CD3 KU Leuven (courtesy of A. Marchand) synthesized the LEDGIN, CX014442[36]. Chemical structures of all compounds are shown in Fig. 1a. Dimethyl

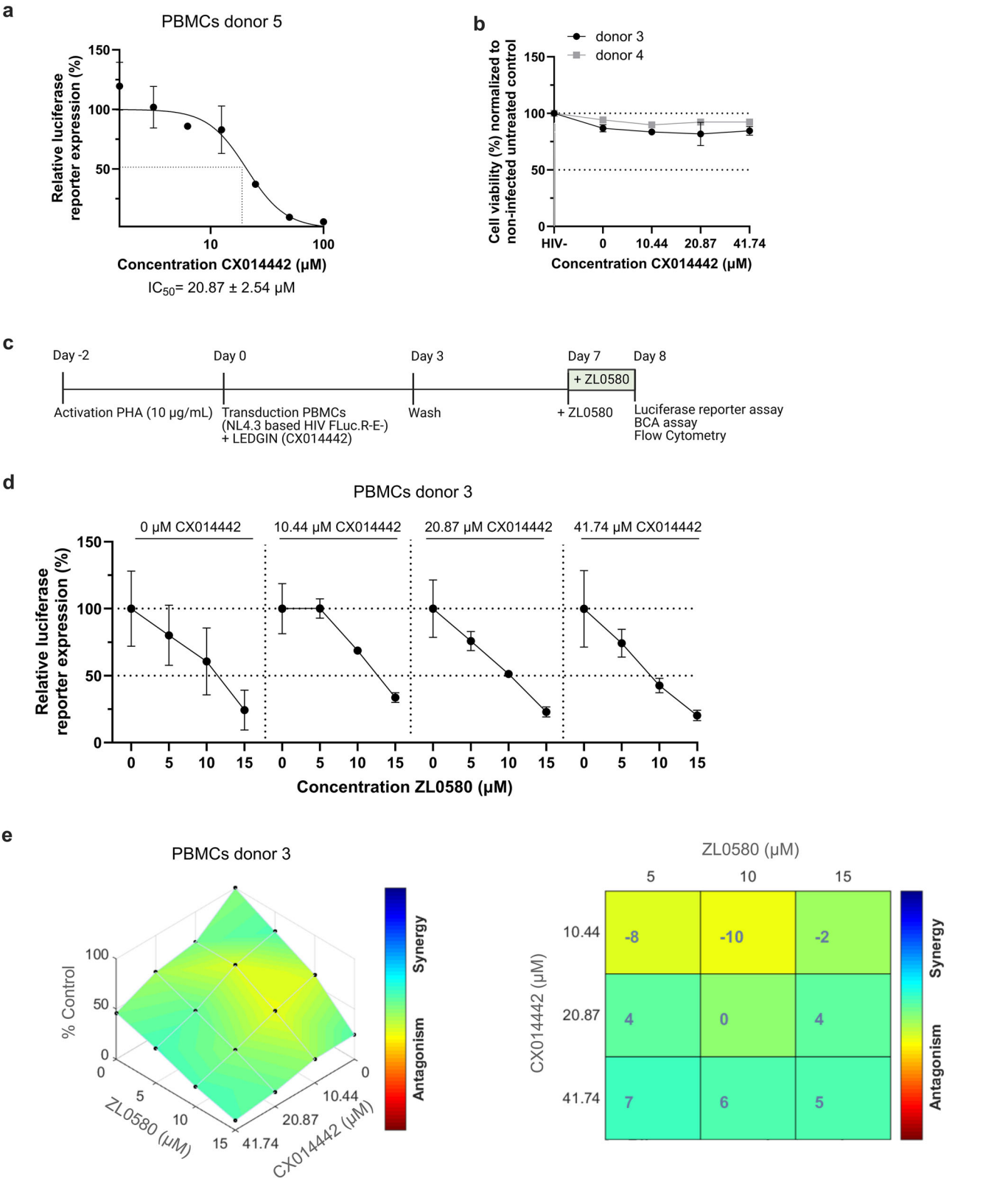

sulfoxide (DMSO; Sigma) was used to dilute all compounds and all compounds were aliquoted and stored at -20 °C to maintain stability.

Transduction, treatment and reactivation of SupT1 cells

3.6×10^5 SupT1 cells were transduced with 2.9×10^4 pg p24 HIV-1 FLuc virus. 3 days after transduction, the cells were washed to remove residual virus and cultured for an additional 7 days to allow silencing of HIV-1 gene expression. At day 10 post-transduction, the cells were treated with a dilution series of JQ1 or ZL0580. Meanwhile, half of these wells were reactivated with 10 ng/mL TNF-α (Immunosource), and the other half remained non-reactivated. Samples were harvested 24 h post-reactivation for the luciferase assay, BCA assay, MTT assay, flow cytometry and bDNA imaging. The timeline of the experiment is summarized in Fig. 1b. Secondly, we investigated the persistence of the

Fig. 8 | LEDGIN CX014442 and ZL0580 additively inhibit HIV-1 transcription in primary cells. a PBMCs were stimulated with 10 µg/mL PHA for 2 days and afterwards transduced with HIV-1 FLuc virus and treated with CX014442 for 3 days. Relative luciferase reporter expression (%) was calculated as luciferase counts (normalized for protein content; BCA assay) relative to the untreated control. The IC_{50}, 20.87 ± 2.54 µM, was determined using a four-parameter logistic regression of a dose-response curve. Mean ± SD of biological duplicates of 1 experiment out of 1 are presented ($n = 2$). **b** On day 3, cells were stained with propidium iodide and analyzed using flow cytometry. Cell viability (%), was calculated relative to the non-transduced negative control (HIV-). Mean ± SD of biological duplicates are presented ($n = 2$; 2 donors). Statistics were not performed due to a limited number of data points. **c** PBMCs from anonymous donors were stimulated with 10 µg/mL PHA for 2 days. The cells were transduced with HIV-1 FLuc virus and treated with a 2-fold dilution series of CX014442 (0.5-2 x IC_{50}) for 3 days. 7 days post-transduction, a dilution series of ZL0580 was added to the cells. 24 h after ZL0580-treatment, samples were harvested for luciferase assay and flow cytometry. **d** On day 8 post-transduction, relative luciferase reporter expression (%) was calculated by normalizing luciferase counts (adjusted for protein content; BCA assay) from ZL0580-treated cells to the control (0 µM ZL0580), separately for each CX014442 concentration. Mean ± SD of biological duplicates are presented ($n = 2$; 4 donors). Statistics were not performed due to a limited number of data points. **e** Using the Combenefit software[56], experimental 3D dose-response curves of the drug combination of CX014442 and ZL0580 were generated, expressed as a percentage of the positive control (0 µM CX014442 and ZL0580). The curve is covered with a color code according to synergy/antagonism scores, calculated with the Bliss Synergy model. The matrix shows the value of the synergy/antagonism scores. The average results from 2 biological duplicates are shown ($n = 2$; 4 donors). Source data are provided in the source data file. IC_{50}, 50% inhibitory concentration; ns, non-significant; PBMCs, peripheral blood mononuclear cells; PHA, phytohemagglutinin; 3D, 3-dimensional.

effect of JQ1 and ZL0580 on HIV-1 transcription by washing away the compound. Therefore, similar infection experiments were conducted as described above, wherein JQ1 or ZL0580 was added on day 10 post-transduction. However, after collecting samples on day 11 post-transduction, the non-reactivated cells were washed and subcultured. On day 12 post-transduction, half of the cells were reactivated with 10 ng/mL TNF-α (Immunosource), while the other half remained non-reactivated. Samples were harvested on day 13 post-transduction for the luciferase assay and flow cytometry. The protocol is outlined in detail in Fig. S4a. Third, we studied the effect of JQ1 and ZL0580 on LEDGIN-retargeted provirus. The experiment was similar as described above, only varying concentrations of LEDGINs were additionally added during transduction with the HIV-1 FLuc virus. Briefly, the residual virus and LEDGINs were washed away on day 3 post-transduction. On day 10 post-transduction, all cells were treated with JQ1 or ZL0580, while half of these cells were additionally reactivated with 10 ng/mL TNF-α (Immunosource). Finally, samples were collected 24 h post-reactivation for the luciferase assay, BCA assay and flow cytometry. The timeline is presented in Fig. 3b. Fourth, we studied the persistence of the combined treatment of JQ1/ZL0580 with LEDGINs. The experiment was similar as described above. Varying concentrations of LEDGINs were added during transduction and residual virus and LEDGINs were washed away on day 3 post-transduction. On day 10 post-transduction, all cells were treated with JQ1 or ZL0580, while half of these cells were additionally reactivated with 10 ng/mL TNF-α (Immunosource). However, after collecting samples for the luciferase assay and flow cytometry on day 11 post-transduction, the non-reactivated cells were washed and subcultured. On day 12 post-transduction, half of the cells were reactivated with 10 ng/mL TNF-α (Immunosource), while the other half remained non-reactivated. Samples were harvested on day 13 post-transduction for the luciferase assay, BCA assay and flow cytometry. The timeline is presented in Fig. S10a.

HIV-1 luciferase reporter assay

Cells were harvested and washed 3 times with phosphate buffered saline (PBS) and subsequently lysed with a home-made lysis buffer (50 mM Tris-HCl pH 7.5, 200 mM NaCl, 0.2% (v/v) NP40 and 5% (v/v) glycerol). After a freeze-thaw cycle, cell lysates were centrifuged (1250 × *g*, 10 min) and 5 µL of the supernatant was mixed with 25 µL of a FLUC assay reagent (ONE-Glow; Promega GMBH). The bioluminescent signal was measured with an Envision 2105 (PerkinElmer). The luciferase counts were normalized for the total protein content per well determined with the BCA assay (BCA protein assay kit; Thermo Scientific). Data are presented as such or the relative luciferase reporter expression (%) was calculated by dividing the luciferase counts normalized for protein content (BCA assay) from the compound-treated wells by those from the untreated positive control.

Propidium iodide staining

Cells were harvested at multiple days for flow cytometry. Cells were stained with 5 µg/mL propidium iodide (Sigma) dye for 15 min at RT. To determine cell viability an 488 nm laser and 774/26 nm bandpass filter was used. As cell viability is assessed, debris was not excluded. 10.000 events were counted and a flow speed of 200 µL/min was used. Every sample is analyzed in biological duplicates. Data was analyzed with the Attune cytometric software software (version 5.2.0) and FCS express (version 7 research edition).

MTT assay

To determine viability, MTT is reduced to a purple formazan derivative by metabolically active intracellular mitochondrial dehydrogenases[87]. In a 96 well plate 1.8×10^5 SupT1 cells were treated with serial dilutions of compound (0-100 µM). After 24 h, 20 µL of the yellow dye, 3-(4,5-dimethylthiazol-2-yl)-2,5-diphenyltetrazolium bromide (MTT) (Sigma), was added to the cells. Afterwards formazan crystals were dissolved by adding 100 µL of an isopropanol solution supplemented with 6% (v/v) Triton and 0.4% (v/v) mL HCl. Two h later, formazan absorbance was measured spectrophotometrically at 540 nm and background at 690 nm by using the Envision 2105 (PerkinElmer). Data are presented as cell viability (%), normalized to the untreated positive control.

Treatment and reactivation of J-Lat A2 cells

In the first experiment, J-Lat A2 cells were plated in a 96-well and treated with a dilution series of ZL0580 and DMSO as a negative control. Meanwhile cells were reactivated with 10 ng/mL TNF-α (Immunosource). After 24 h, samples were harvested for flow cytometry. Cells were stained with 1/1000 dilution of eBioscience fixable viability dye 780 (Invitrogen) for 30 min at 4 °C and afterwards fixated with 4% perfluoroalkyl solution (PFA; Alfa Aesar) for 15 min. The protocol is outlined in detail in Fig. S3a.

Flow cytometric analysis of J-LatA2 cells

To determine cell viability a 537 nm laser and a 775/50 nm bandpass filter was used. Doublets were excluded using the FSC-A/FSC-H. In parallel, GFP expression was determined with the Invitrogen Attune NxT Flow Cytometry (Thermo Fisher Scientific) using a 488 nm excitation laser and 525/50 nm band pass filter. Live cells were gated using the forward and side scatter channel (FSC-A/SSC-A) and doublets were excluded (FSC-A/FSC-H). Gating strategy is presented in Fig. S3b. 10.000 events were counted and a flow speed of 200 µL/min was used. Every sample is analyzed in biological duplicates. Data were analyzed with the Attune cytometric software (version 5.2.0) and FCS express software (version 7 research edition).

https://doi.org/10.1038/s41467-025-59398-7

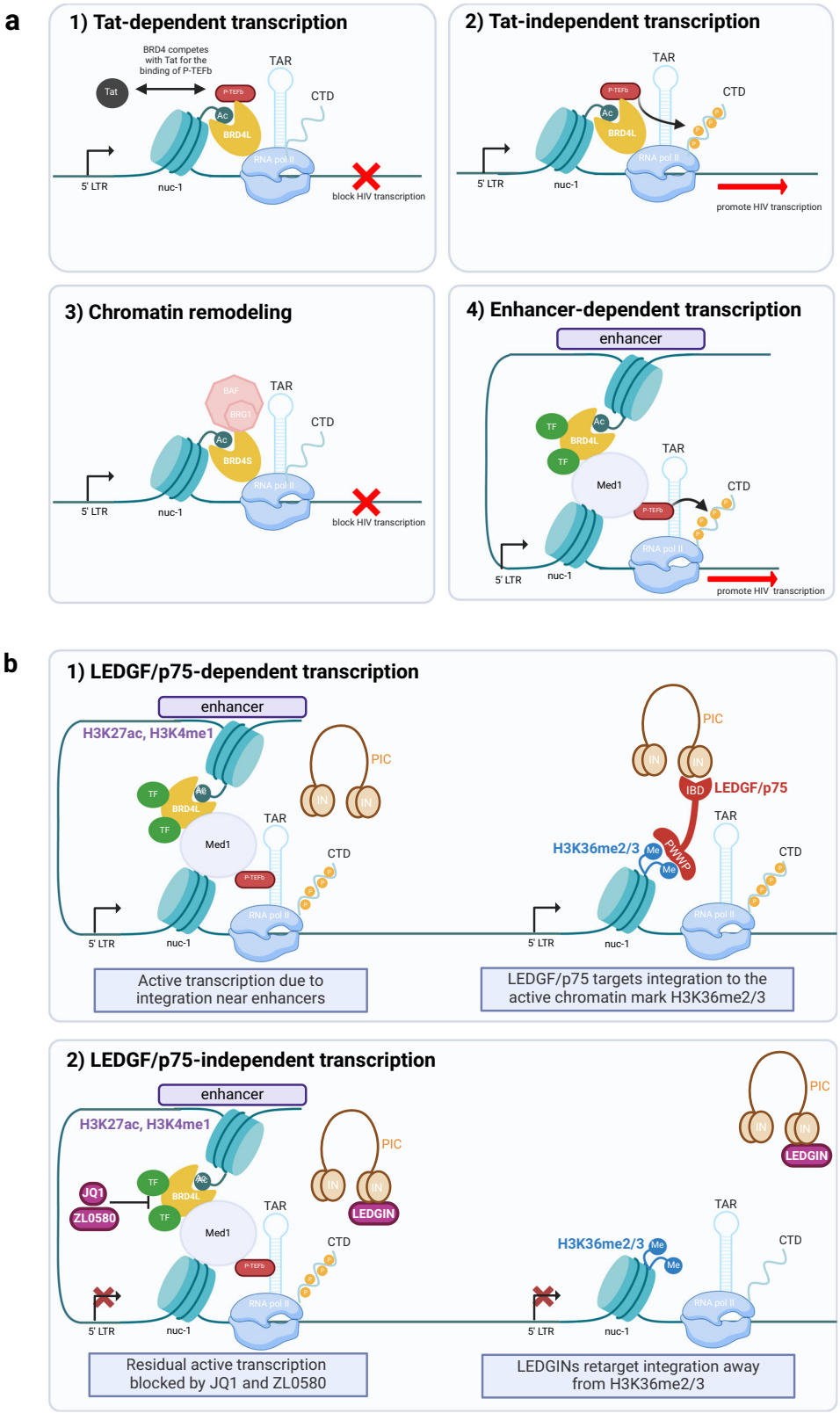

Tat assay

20×10^5 HeLa-derived TZM-bl cells, that express CD4/CCR5 and contain Tat-inducible FLuc and beta-Gal reporter genes[83], were plated in a 96-well. 24 h later, following a wash step with PBS, the cells were transfected with 1000 ng Tat plasmid (NIH HIV Reagent Program) with the use of lipofectamine 3000 (Invitrogen). One day after transfection, cells were treated with ZL0580 and JQ1 for 24 h. Cells were harvested for the luciferase and BCA assays.

Branched-DNA imaging

The bDNA assay performed with the RNA scope technology (Advance Cell Diagnostics)[88] was optimized by Puray-Chavez et al.[89]. After HIV-1

Fig. 9 | The role of BRD4 in HIV-1 transcription in LEDGF/p75-dependent and LEDGIN-retargeted provirus. BRD4 affects HIV-1 transcription at multiple levels. (1) BRD4 is a negative regulator of Tat-dependent transcription. BRD4 is bound to acetylated histones and competitively blocks the interaction of Tat with P-TEFβ preventing the formation of the Super elongation complex (SEC). (2) BRD4 is a positive regulator of Tat-independent transcription because BRD4 recruits P-TEFβ to the viral promotor. (3) BRD4 blocks HIV-1 transcription through BRG1. The short isoform of BRD4, lacking a P-TEFb interaction domain, directly binds BRG1 and acetylated histones, resulting in a recruitment of BRG1 to the HIV-1 promotor. BRG1 is a catalytical subunit of BAF, **a** SWI/SNF chromatin-remodeling complex which induces a repressive promotor nucleosome position. (4) BRD4 mediates enhancer-dependent transcription in *trans* leading to the further recruitment of P-TEFβ, Med1 and transcription factors (TFs). **b** LEDGF/p75 contains an IBD that binds the viral IN and a PWWP domain that binds the active chromatin mark, H3K36me2/3. LEDGF/p75 targets integration into active genes. Active transcription can also result from a stochastic integration near enhancer regions (with H3K27ac or H3K4me1 as marks), independent of LEDGF/p75 but dependent on BRD4. LEDGINs bind the LEDGF/p75 binding pocket of the viral integrase and retarget integration away from H3K36me2/3 into repressive chromatin regions but do not influence the proximity of integration near enhancer regions. Residual active transcription after LEDGIN-treatment may be caused by integration near enhancers. BRD4 modulators, like JQ1 and ZL0580, may silence enhancer-dependent transcription after LEDGIN-treatment. Figure adapted from[41] and created in BioRender. Van belle, S. (2025) https:// BioRender.com/3jlc8r. Ac, acetylated; BAF, brahma associated factor; BRD4L, bromodomain containing protein 4 long isoform; BRD4S, bromodomain containing protein 4 short isoform; BRG1, brahma related gene 1; CTD, carboxy terminal domain; ELLII, elongation factor for RNA Pol II; IBD, integrase binding domain; IN, integrase; Med1, mediator complex subunit 1; pol, polymerase; PIC, pre-integration complex; P-TEFβ, positive transcription elongation factor β; SEC, super elongation complex; TAR, trans-activation response element; Tat, trans-activator of transcription; TF, transcription factors; 7SK snRNP, 7SK small nuclear ribonucleoprotein.

transduction and reactivation, cells were adhered to a Poly-D-Lysine cover slip (Neuvitro) and fixed with a 4% (v/v) PFA (Alfa Aesar). After fixation, the cells were dehydrated using increasing concentrations of ethanol (0%, 50%, 70%, and 100% (v/v); Fisher Scientific) and stored at -20 °C. After storage, the cells were rehydrated with 70%, 50%, and 0% (v/v) ethanol solutions and permeabilized with 0.1% (v/v) tween-20 (Thermo Fisher Scientific). For vRNA detection, a vRNA probe targeting the non-*Gag/Pol* region of the HIV-1 genome (REF317711-C2; Advanced Cell Diagnostics) was added to the cells, diluted in a 1:50 ratio (v/v) with probe diluent (REF 300041: Advanced Cell Diagnostics). Subsequently, vDNA detection took place with a sense HIV-Gag/Pol-C1 probe (REF 317701, Advanced Cell Diagnostics). For signal amplification, amplifiers were added, which are conjugated with a fluorophore (ATTO 550 for vDNA, pseudocolored red in the images; ATTO 635 for vRNA, pseudocolored green in the images) to hybridize to the probes. Further, to visualize the nucleus, a 4′,6-diamidino-2-phenylindole (DAPI; 0.001 µg/µL; Life Technologies) staining was performed. After bDNA hybridization, the fluorescent signals of DAPI, the vRNA probe (635 fluorophore), and the vDNA probe (550 fluorophore) were detected with fluorescence confocal microscopy (FLUOVIEW FV1000 or FV2000, Olympus) with a UPLSAPO 60x water-immersion objective. The excitation wavelengths of the lasers for DAPI, the vRNA probe, and the vDNA probe were set at 405, 635 and 559 nm, respectively. Using a 0.3 µm step size and 4 µs/pixel sampling speed, 3-dimensional stacks were taken. After acquiring the images of the DAPI, vRNA, and vDNA signal, the images were converted to tiff files via Fiji using a home-written Fiji routine. These tiff files were further used in the in-house designed MATLAB routine, adapted from Crocker et al.[90], to quantify the vDNA and vRNA spots at a single-cell level.

Co-localization between BRD4 and lysine acetylation in histone

To investigate the effect of the compounds on co-localization between BRD4 and acetylated lysines (KAc) in the histones, confocal microscopy was used. First, chambers were pretreated with poly-D-lysine (Sigma-Aldrich), and 3.75×10^5 SupT1 cells were plated into an 8-well chamber slide. Next, the cells were incubated with JQ1 (1, 5 µM), ZL0580 (3.4, 5 µM) or left untreated for 24 h. Afterwards, the cells were fixed with 4% (v/v) PFA (Alfa Aesar) for 10 min and permeabilized with 0.2% (v/v) Triton-X-100 (Arcos Organics) and 2% (v/v) bovine serum albumin (BSA; Sigma-Aldrich) in PBS for 30 min. After washing the cells 3 times, a blocking buffer containing 10% (v/v) FBS (GIBCO) and 0.2% (v/v) Tween-20 (Fisher Scientific) in PBS was added for 15 min. Overnight, the cells were stained at 4 °C with the primary antibodies: anti-BRD4 1:100 (Santa Cruz, sc-518021), anti-BRD4 1:100 (Abcam, ab128874, lot GR3251918-2), anti-H3K9/14Ac 1:2000 (Diagenode, C15410200), anti-H4K8Ac 1:100 (Invitrogen, GT478, lot ZG4382220) diluted in blocking buffer. The cells were washed 3 times with PBS and incubated for 3 h with secondary antibodies: Goat Anti-Mouse IgG conjugated with Alexa488 (Invitrogen, A11001, lot2714439) 1:500, F(ab')2-Goat anti-Rabbit IgG (H + L) Cross-Adsorbed Secondary Antibody Alexa Fluor 488 (Invitrogen, A11070, lot 2896481) 1:1000, Goat Anti-Rabbit IgG conjugated with Alexa633 (Invitrogen, 40839) 1:500, Goat anti-Mouse IgG (H + L) Cross-Adsorbed Secondary Antibody Alexa Fluor™ 633 (Invitrogen, A-21050, lot 2540908) 1:1000 in blocking buffer supplemented with 5% (v/v) goat serum. Finally, the cells were incubated with blocking buffer supplemented with 1:5000 DAPI (Life Technologies) for 5 min to stain the nucleus. Afterwards the slides were washed with PBS. Fluorescence images were acquired using a laser scanning microscope LSM 880 – Airyscan (Carl Zeiss) with the 63X oil-immersion objective. Lasers with 405, 488, 630 nm excitation beams were used. The degree of co-localization was quantified via PCC using Fiji (ImageJ).

Combenefit synergy calculations

Analysis and data visualization of synergy of drug combinations were performed using Combenefit Software (version 2.021 for Microsoft) (University of Cambridge), downloaded at https://sourceforge.net/projects/combenefit/[56]. The luciferase reporter data are normalized to the untreated positive control (%). From the latter, dose-response curves of both single compounds and an experimental dose-response surface of the combination of both compounds are generated. Afterwards, a reference dose-response surface is produced by the software based on the dose-response curve of the single compounds. Combenefit provides the choice between 3 models to generate this reference dose-response surface. Based on literature research of the 3 models, the Bliss model was applied to our data because it is considered suitable for assessing the effects of drugs with different mechanisms of action[91–93]. By comparing the experimental dose-response surface to the reference dose-response curve a synergy/ antagonism score is shown for each drug combination tested.

Isolation of primary cells

Using a Lymphoprep density gradient (Stem Cell Technologies), human PBMCs were purified from buffy coats received from the Red Cross Blood Transfusion Center (Mechelen; Belgium) and afterwards stored in liquid nitrogen until use. The experiments with human blood cells received bioethical approval by the Medical Ethics committee of the KU Leuven (S69957).

Infection and activation of primary cells

PBMCs were stimulated with 10 µg/mL PHA (Sigma) 2 days before transduction. These cells were transduced with 1.73×10^6 pg p24 HIV-1 FLuc virus per 1×10^6 cells. 3 days post-transduction, residual virus was washed away and cells were subcultured for an additional 4 days. At day 7 post-transduction, the cells were treated with a dilution series of

ZL0580. 24 h post-treatment, samples were collected for the luciferase assay. In addition, cells were washed to remove the compound and subcultured. 1, 2 and 3 days after removal of ZL0580, samples were harvested for the luciferase assay as well. The timeline is presented in detail in Fig. 6a. Second, we investigated the effect of multiple treatments with ZL0580 in PBMCs. The experiment was similar as described above. But between the washing step on day 3 post-transduction and the treatment with ZL0580 on day 7 post-transduction, PBMCs were additionally pretreated once or twice with ZL0580. The timeline is shown in Fig. 7a and b. Third, we studied the effect of ZL0580 on LEDGIN-retargeted proviruses in primary cells. Therefore, varying concentrations of LEDGINs were added during transduction. The experiment was similar as described above. Briefly, the residual virus and LEDGINs were washed away on day 3 post-transduction. On day 7 post-transduction, cells were treated with varying concentrations of ZL0580. Finally, samples were collected 24 h after ZL0580-treatment for the luciferase assay. The timeline is presented in Fig. 8c. Fourth, we studied the persistence of the combined treatment of LEDGIN and ZL0580 in primary cells. The experiment was similar as described above. But in addition to harvesting samples for the luciferase assay at day 7 after transduction, cells were washed to remove the compound and subcultured. 1, 2, and 3 days after removal of ZL0580, samples were harvested for the luciferase assay as well. The timeline is presented in detail in Fig. S13a.

Statistical analysis

Using GraphPad Prism software (version 10.00 for Microsoft) (www.graphpad.com), a non-linear regression curve fit of a dose-response curve was used to determine the CC_{50} and IC_{50} values of the compounds. Statistical significance was calculated using GraphPad Prism with a One-way ANOVA, a Brown-Forsythe and Welch ANOVA or a Kruskal-Wallis test, depending on the normality test (Normality test of D'Agostino, Anderson-Darling, Shapiro-Wilk, Kolmogorov-Smirnov) and the equality of the group variances (Brown-Forsythe and Barlett's test). Tests were corrected for multiple comparisons with the Sidak's multiple comparison test, s multiple comparison test, Dunnett's T3 multiple comparison test or the Dunn's multiple comparison test. SPSS software (version 30 for Microsoft) was applied to conduct the negative binomial probability distribution on the data generated with bDNA imaging. The deviance (goodness of fit coefficient) was 0.572 (CX014442, SupT1 cells), 0.956 (JQ1, SupT1 cells) and 0.620 (ZL0580, SupT1 cells). Statistical significance is noted as: ns non-significant; * $p < 0.05$; ** $p < 0.01$; *** $p < 0.0001$; **** $p < 0.0001$).

Reporting summary

Further information on research design is available in the Nature Portfolio Reporting Summary linked to this article.

Data availability

Source data are provided with this paper.

References

1. Chen, J. et al. The reservoir of latent HIV. *Front. Cell. Infect. Microbiol.* **12**, 1–15 (2022).
2. Younas, M. et al. Residual viremia is linked to a specific immune activation profile in HIV-1-infected adults under efficient antiretroviral therapy. *Front. Immunol.* **12**, 1–9 (2021).
3. Abner, E. & Jordan, A. HIV "shock and kill" therapy: In need of revision. *Antiviral Res.* **166**, 19–34 (2019).
4. Janssens, J., Bruggemans, A., Christ, F. & Debyser, Z. Towards a Functional Cure of HIV-1: Insight into the chromatin landscape of the provirus. *Front. microbiol.* **12**, 636642 (2021).
5. Debyser, Z., Vansant, G., Bruggemans, A., Janssens, J. & Christ, F. Insight in HIV integration site selection provides a block-and-lock strategy for a functional cure of HIV infection. *Viruses* **11**, 1–12 (2019).
6. Moranguinho, I. & Valente, S. T. Block-and-lock: New horizons for a cure for hiv-1. *Viruses* **12**, (2020).
7. Ahlenstiel, C. L., Symonds, G., Kent, S. J. & Kelleher, A. D. Block and lock HIV cure strategies to control the latent reservoir. *Front. Cell. Infect. Microbiol.* **10**, 1–13 (2020).
8. Vansant, G., Bruggemans, A., Janssens, J. & Debyser, Z. Block-and-lock strategies to cure HIV infection. *Viruses* **12**, 1–17 (2020).
9. Mediouni, S. et al. Didehydro-cortistatin a inhibits HIV-1 by specifically binding to the unstructured basic region of tat. *mBio* **10**, 1–19 (2019).
10. Castro-Gonzalez, S., Colomer-Lluch, M. & Serra-Moreno, R. Barriers for HIV Cure: The latent reservoir. *AIDS Res. Hum. Retroviruses* **34**, 739–759 (2018).
11. Kim, Y., Anderson, J. L. & Lewin, S. R. Getting the "kill" into "shock and kill": strategies to eliminate latent HIV. *Cell Host Microbe* **1**, 14–26 (2018).
12. Darcis, G., Van Driessche, B. & Van Lint, C. HIV Latency: Should we shock or lock? *Trends Immunol* **38**, 217–228 (2017).
13. Dahabieh, M. S., Battivelli, E. & Verdin, E. Understanding HIV latency: The road to an HIV cure. *Annu. Rev. Med.* **66**, 407–421 (2015).
14. Søgaard, O. S. et al. The depsipeptide romidepsin reverses HIV-1 latency in vivo. *PLoS Pathog* **11**, 1–22 (2015).
15. Archin, N. M. et al. Administration of vorinostat disrupts HIV-1 latency in patients on antiretroviral therapy. *Nature* **487**, 482–485 (2012).
16. Matalon, S., Rasmussen, T. A. & Dinarello, C. A. Histone deacetylase inhibitors for purging HIV-1 from the latent reservoir. *Mol. Med.* **17**, 466–472 (2011).
17. Van Lint, C., Bouchat, S. & Marcello, A. HIV-1 transcription and latency: An update. *Retrovirology* **10**, 1 (2013).
18. Davenport, M. P. et al. Functional cure of HIV: the scale of the challenge. *Nat. Rev. Immunol.* **19**, 45–54 (2019).
19. Mousseau, G. et al. An Analog of the natural steroidal alkaloid cortistatin a potently suppresses tat-dependent HIV transcription. *Cell Host Microbe* **12**, 97–108 (2012).
20. Mousseau, G. et al. The tat inhibitor didehydro-cortistatin a prevents HIV-1 reactivation from latency. *mBio* **6**, 1–14 (2015).
21. Ott, M., Geyer, M. & Zhou, Q. The control of HIV transcription: Keeping RNA polymerase II on track. *Cell Host Microbe* **10**, 426–435 (2011).
22. Kessing, C. F. et al. In vivo suppression of HIV rebound by didehydro-Cortistatin A, a "block-and-lock" strategy for HIV-1 cure. *Cell Rep.* **21**, 600–611 (2017).
23. Li, C., Mousseau, G. & Valente, S. T. Tat inhibition by didehydro-Cortistatin A promotes heterochromatin formation at the HIV-1 long terminal repeat. *Epigenetics Chromatin* **12**, 1–17 (2019).
24. Blokken, J., De Rijck, J., Christ, F. & Debyser, Z. Protein–protein and protein–chromatin interactions of LEDGF/p75 as novel drug targets. *Drug Discov. Today Technol.* **24**, 25–31 (2017).
25. Llano, M. et al. Identification and characterization of the chromatin-binding domains of the HIV-1 integrase interactor LEDGF/p75. *J. Mol. Biol.* **360**, 760–773 (2006).
26. Marshall, H. M. et al. Role of PSIP1/LEDGF/p75 in lentiviral infectivity and integration targeting. *PLoS ONE* **2**, 10.1371/journal.-pone.0001340 (2007).
27. Shun, M. C. et al. LEDGF/p75 functions downstream from preintegration complex formation to effect gene-specific HIV-1 integration. *Genes Dev* **21**, 1767–1778 (2007).
28. Ciuffi, A. et al. A role for LEDGF/p75 in targeting HIV DNA integration. *Nat. Med.* **11**, 1287–1289 (2005).

29. Meehan, A. M. et al. LEDGF/p75 proteins with alternative chromatin tethers are functional HIV-1 cofactors. *PLoS Pathog*. **5**, e1000522 (2009).
30. Gijsbers, R. et al. LEDGF hybrids efficiently retarget lentiviral integration into heterochromatin. *Mol Ther*. **18**, 552–560 (2010).
31. Acke, A. et al. Expansion microscopy allows high resolution single cell analysis of epigenetic readers. *Nucleic Acids Res*. **50**, e100–e100 (2022).
32. Christ, F. & Debyser, Z. The LEDGF/p75 integrase interaction, a novel target for anti-HIV therapy. *Virology* **435**, 102–109 (2013).
33. Vandekerckhove, L. et al. Transient and stable knockdown of the integrase cofactor LEDGF/p75 reveals its role in the replication cycle of human immunodeficiency virus. *J. Virol.* **80**, 1886–1896 (2006).
34. De Rijck, J. et al. Overexpression of the lens epithelium-derived growth factor/p75 integrase binding domain inhibits human immunodeficiency virus replication. *J. Virol.* **80**, 11498–11509 (2006).
35. Christ, F. et al. Rational design of small-molecule inhibitors of the LEDGF/p75-integrase interaction and HIV replication. *Nat. Chem. Biol.* **6**, 442–448 (2010).
36. Christ, F. et al. Small-molecule inhibitors of the LEDGF/p75 binding site of integrase block HIV replication and modulate integrase multimerization. *Antimicrob. Agents Chemother.* **56**, 4365–4374 (2012).
37. Tsiang, M. et al. New class of HIV-1 integrase (IN) inhibitors with a dual mode of action. *J. Biol. Chem.* **287**, 21189–21203 (2012).
38. Vranckx, L. S. et al. LEDGIN-mediated Inhibition of Integrase-LEDGF/p75 Interaction Reduces Reactivation of Residual Latent HIV. *EBioMedicine* **8**, 248–264 (2016).
39. Desimmie, B. A. et al. LEDGINs inhibit late stage HIV-1 replication by modulating integrase multimerization in the virions. *Retrovirology* **17**, 1–16 (2020).
40. Vansant, G. et al. Impact of LEDGIN treatment during virus production on residual HIV-1 transcription. *Retrovirology* **16**, 1–17 (2019).
41. Vansant, G. et al. The chromatin landscape at the HIV-1 provirus integration site determines viral expression. *Nucleic Acids Res*. **48**, 7801–7817 (2020).
42. Janssens, J., De Wit, F., Parveen, N. & Debyser, Z. Single-Cell Imaging Shows That the transcriptional state of the HIV-1 Provirus and Its Reactivation Potential Depend on the Integration Site. *mBio* https://doi.org/10.1128/mbio.00007-22 (2022).
43. Bruggemans, A. et al. GS-9822, a preclinical LEDGIN candidate, displays a block-and- lock phenotype in cell culture. *Antimicrob. Agents Chemother.* **65**, 1–17 (2021).
44. Rahnamoun, H. et al. RNAs interact with BRD4 to promote enhanced chromatin engagement and transcription activation. *Nat. Struct. Mol. Biol.* **25**, 687–697 (2018).
45. Lovén, J. et al. Selective inhibition of tumor oncogenes by disruption of super-. *Enhancers. Cell* **153**, 320–334 (2013).
46. Li, Z., Guo, J., Wu, Y. & Zhou, Q. The BET bromodomain inhibitor JQ1 activates HIV latency through antagonizing Brd4 inhibition of Tat-transactivation. *Nucleic Acids Res*. **41**, 277–287 (2013).
47. Bartholomeeusen, K., Xiang, Y., Fujinaga, K. & Peterlin, B. M. Bromodomain and extra-terminal (BET) bromodomain inhibition activate transcription via transient release of Positive Transcription Elongation Factor b (P-TEFb) from 7SK small nuclear ribonucleoprotein. *J. Biol. Chem.* **287**, 36609–36616 (2012).
48. Zhu, J. et al. Reactivation of latent HIV-1 by inhibition of BRD4. *Cell Rep.* **2**, 807–816 (2012).
49. Boehm, D. et al. BET bromodomain-targeting compounds reactivate HIV from latency via a Tat-independent mechanism. *Cell Cycle* **12**, 452–462 (2013).
50. Bisgrove, D. A., Mahmoudi, T., Henklein, P. & Verdin, E. Conserved P-TEFb-interacting domain of BRD4 inhibits HIV transcription. *Proc. Natl. Acad. Sci. USA.* **104**, 13690–13695 (2007).
51. Niu, Q. et al. Structure-guided drug design identifies a BRD4-selective small molecule that suppresses HIV. *J. Clin. Invest.* **129**, 3361–3373 (2019).
52. Alamer, E. et al. Epigenetic suppression of HIV in myeloid cells by the BRD4- selective small molecule modulator ZL0580. *J. Virol* **94**, 1880–19 (2020).
53. Alamer, E., Zhong, C., Hajnik, R., Soong, L. & Hu, H. Modulation of BRD4 in HIV epigenetic regulation: implications for finding an HIV cure. *Retrovirology* **18**, 1–9 (2021).
54. Filippakopoulos, P. et al. Histone recognition and large-scale structural analysis of the human bromodomain family. *Cell* **149**, 214–231 (2012).
55. Filippakopoulos, P. et al. Selective inhibition of BET bromodomains. *Nature* **468**, 1067–1073 (2010).
56. Di Veroli, G. Y. et al. Combenefit: An interactive platform for the analysis and visualization of drug combinations. *Bioinformatics* **32**, 2866–2868 (2016).
57. Urano, E. et al. Identification of the P-TEFb complex-interacting domain of Brd4 as an inhibitor of HIV-1 replication by functional cDNA library screening in MT-4 cells. *FEBS Lett* **582**, 4053–4058 (2008).
58. Banerjee, C. et al. BET bromodomain inhibition as a novel strategy for reactivation of HIV-1. *J. Leukoc. Biol.* **92**, 1147–1154 (2012).
59. Yang, Z. et al. Recruitment of P-TEFb for stimulation of transcriptional elongation by the bromodomain protein Brd4. *Mol. Cell* **19**, 535–545 (2005).
60. Moon, K. J. et al. The bromodomain protein Brd4 is a positive regulatory component of P-TEFb and stimulates RNA polymerase II-dependent transcription. *Mol. Cell* **19**, 523–534 (2005).
61. Zhou, Q. & Yik, J. H. N. The yin and yang of P-TEFb Regulation: Implications for human immunodeficiency virus gene expression and global control of cell growth and differentiation. *Microbiol. Mol. Biol. Rev.* **70**, 646–659 (2006).
62. Schröder, S. et al. Two-pronged binding with bromodomain-containing protein 4 liberates positive transcription elongation factor b from inactive ribonucleoprotein complexes. *J. Biol. Chem.* **287**, 1090–1099 (2012).
63. Krueger, B. J., Varzavand, K., Cooper, J. J. & Price, D. H. The mechanism of release of P-TEFb and HEXIM1 from the 7SK snRNP by viral and cellular activators includes a conformational change in 7SK. *PLoS ONE* **5**, e12335 (2010).
64. Conrad, R. J. et al. The short isoform of BRD4 Promotes HIV-1 latency by engaging repressive SWI/SNF chromatin remodeling complexes. *Mol Cell* **67**, 1001–1012 (2018).
65. Lucic, B. et al. Spatially clustered loci with multiple enhancers are frequent targets of HIV-1 integration. *Nat. Commun.* **10**, 1–12 (2019).
66. Huang, B., Yang, X.-D., Zhou, M.-M., Ozato, K. & Chen, L.-F. Brd4 Coactivates Transcriptional Activation of NF-κB via Specific Binding to Acetylated RelA. *Mol. Cell. Biol.* **29**, 1375–1387 (2009).
67. Zou, Z. et al. Brd4 maintains constitutively active NF-κB in cancer cells by binding to acetylated RelA. *Oncogene* **33**, 2395–2404 (2014).
68. Hajmirza, A. et al. BET Family Protein BRD4: An Emerging Actor in NFκB Signaling in Inflammation and Cancer. *Biomedicines* **6**, 16 (2018).
69. Janssens, J. et al. Mechanisms and efficacy of small molecule "latency promoting agents" to inhibit HIV reactivation ex vivo. *JCI Insight* https://doi.org/10.1172/jci.insight.183084 (2024).
70. Verdin, E., Paras, P. & Vanlint, C. Chromatin disruption in the promoter of HIV-1 during transcriptional activation. *Embo* **12**, 3249–3259 (1993).

71. Van Lint, C., Emiliani, S., Ott, M. & Verdin, E. Transcriptional activation and chromatin remodeling of the HIV-1 promoter in response to histone acetylation. *The em* **15**, 1112–1120 (1996).
72. Chen, H. C., Martinez, J. P., Zorita, E., Meyerhans, A. & Filion, G. J. Position effects influence HIV latency reversal. *Nat. Struct. Mol. Biol.* **24**, 47–54 (2017).
73. Padmanabhan, B., Mathur, S., Manjula, R. & Tripathi, S. Bromodomain and extra-terminal (BET) family proteins: New therapeutic targets in major diseases. *J. Biosci.* **41**, 295–311 (2016).
74. Ameratunga, M. et al. First-in-human Phase 1 open label study of the BET inhibitor ODM-207 in patients with selected solid tumours. *Br. J. Cancer* **123**, 1730–1736 (2020).
75. Shorstova, T., Foulkes, W. D. & Witcher, M. Achieving clinical success with BET inhibitors as anti-cancer agents. *Br. J. Cancer* **124**, 1478–1490 (2021).
76. Farhadian, S. F. et al. HIV viral transcription and immune perturbations in the CNS of people with HIV despite ART. *JCI Insight* **7**, 1–15 (2022).
77. Brodin, J. et al. Establishment and stability of the latent HIV-1 DNA reservoir. *eLife* **5**, e18889 (2016).
78. Abrahams, M.-R. et al. The replication-competent HIV-1 latent reservoir is primarily established near the time of therapy initiation. *Sci. Transl. Med.* **11**, eaaw5589 (2019).
79. Pellaers, E., Denis, A. & Debyser, Z. New latency-promoting agents for a block-and-lock functional cure strategy. *Curr. Opin. HIV AIDS* **19**, 95–101 (2024).
80. Ablashi, D. V. et al. Human herpesvirus-7 (HHV-7): current status. *Clin. Diagn. Virol.* **4**, 1–13 (1995).
81. Jordan, A. HIV reproducibly establishes a latent infection after acute infection of T cells in vitro. *EMBO J* **22**, 1868–1877 (2003).
82. Mondor, I., Ugolini, S. & Sattentau, Q. J. Human immunodeficiency virus type 1 attachment to hela CD4 cells is CD4 Independent and gp120 dependent and requires cell surface heparans. *J. Virol.* **72**, 3623–3634 (1998).
83. Platt, E. J., Bilska, M., Kozak, S. L., Kabat, D. & Montefiori, D. C. Evidence that ecotropic murine leukemia virus contamination in TZM-bl cells does not affect the outcome of neutralizing antibody assays with human immunodeficiency virus type 1. *J. Virol.* **83**, 8289–8292 (2009).
84. Adachi, A. et al. Production of acquired immunodeficiency syndrome-associated retrovirus in human and nonhuman cells transfected with an infectious molecular clone. *J. Virol.* **59**, 284–291 (1986).
85. Ibrahimi, A. et al. Highly efficient multicistronic lentiviral vectors with peptide 2A sequences. *Human Gene Therapy.* **20**, 845–860 (2009).
86. Geraerts, M., Micheils, M., Baekelandt, V., Debyser, Z. & Gijsbers, R. Upscaling of lentiviral vector production by tangential flow filtration. *J. Gene Med.* **7**, 1299–1310 (2005).
87. Pannecouque, C., Daelemans, D. & De Clercq, E. Tetrazolium-based colorimetric assay for the detection of HIV replication inhibitors: Revisited 20 years later. *Nat. Protoc.* **3**, 427–434 (2008).
88. Wang, F. et al. RNAscope: A novel in situ RNA analysis platform for formalin-fixed, paraffin-embedded tissues. *J. Mol. Diagn.* **14**, 22–29 (2012).
89. Puray-Chavez, M. et al. Multiplex single-cell visualization of nucleic acids and protein during HIV infection. *Nat. Commun.* **8**, 1–11 (2017).
90. Crocker, J. & Grier, D. Methods of digital video microscopy for colloidal studies | Elsevier enhanced reader. *J. Colloid Interface Sci.* **179**, 298–310 (1995).
91. Roell, K. R., Reif, D. M. & Motsinger-Reif, A. A. An introduction to terminology and methodology of chemical synergy-perspectives from across disciplines. *Front. Pharmacol.* **8**, 1–11 (2017).
92. Sinzger, M., Vanhoefer, J., Loos, C. & Hasenauer, J. Comparison of null models for combination drug therapy reveals Hand model as biochemically most plausible. *Sci. Rep.* **9**, 1–15 (2019).
93. Yadav, B., Wennerberg, K., Aittokallio, T. & Tang, J. Searching for drug synergy in complex dose-response landscapes using an interaction potency model. *Comput. Struct. Biotechnol. J.* **13**, 504–513 (2015).

Acknowledgements

We thank B. Van Remoortel, M. Smits, and P. Van de Velde (Molecular Virology and Gene Therapy, KU Leuven) for the technical assistance. Funding: Z.D. received funding from the Research Foundation Flanders (FWO) (G023825N) (G091522N), SBO-Saphir (S000319N), and the KU Leuven Research Council (C14/17/095-3M170311) (C14/21/099). Z.P. received funding from the International (Regional) Cooperation and Exchange Project of the National Natural Science Foundation of China (82211530493). E.P. received a personal doctoral fellowship of the FWO (1123025).

Author contributions

Z.D. conceived, designed, and supervised the study. J.J. introduced and optimized branched DNA imaging in the lab and provided insightful feedback. E.P. conceptualized, designed, and performed all the experiments. E.P. analyzed all data and prepared the figures. A.B., L.W., and A.D. provided technical assistance. Z. Peng and F. Da synthesized ZL0580. S.V.B. and C.F. provided logistical and administrative assistance, as well as insightful feedback. E.P. and Z.D. wrote the manuscript. All authors read and approved the final manuscript.

Competing interests

The authors declare no competing interests.

Additional information

Supplementary information The online version contains supplementary material available at https://doi.org/10.1038/s41467-025-59398-7.

Correspondence and requests for materials should be addressed to Zeger Debyser.

Peer review information *Nature Communications* thanks Haitao Hu, and the other, anonymous, reviewer(s) for their contribution to the peer review of this work. A peer review file is available.